Table 1. Proteins of Differential Expression in Mitochondria of Core-Expressing Cells

Protein Name	Fold Change (Mean ± SD)
Increased	
Succinyl-CoA:ketoacid CoA transferase	10.43 ± 1.29
NADH-specific isocitrate dehydrogenase a subunit precursor	9.64 ± 4.66
Unknown	8.65 ± 2.40
GrpE-like protein co-chaperon	5.71 ± 0.49
Leucine aminopeptidase	4.26 ± 1.14
Pyruvate dehydrogenase E1 component b subunit	3.79 ± 1.34
CGO15alt2	3.18 ± 0.80
HSP70	3.11 ± 1.39
Prohibitin	2.60 ± 0.24
3-Hydroxyisobutyrate dehydrogenase	2.47 ± 0.77
HSPC108	2.46 ± 0.69
MnSOD	2.35 ± 0.65
Ubiquinol-cytochrome c oxidoreductase core I protein	2.00 ± 0.23
Decreased	
Aldehyde dehydrogenase 2	0.12 ± 0.02
Aldehyde dehydrogenase 5 precursor	0.25 ± 0.03
ATP synthase a subunit isoform 1	0.50 ± 0.09
Reference protein	
HSP60	1.02 ± 0.02

protein spots was smaller than those reported in a recent study investigating the human placental mitochondrial proteome.[15]

We then compared the intensity of the spots between core-expressing and control cells. Analysis of repeated experiments by Student's t test revealed 13 increased and three decreased spots in intensity in core-expressing cells. These spots were excised and digested with trypsin, then proteins were identified by mass spectrometry. The names of the identified proteins are listed in Table 1. Among them were proteins related to mitochondrial respiratory chain, protein chaperons, and lipid metabolism. Because antibodies to some of these proteins are commercially available, expression levels of the proteins were examined by immunoblotting. The expression levels of the PDH-E1β subunit and MnSOD, which were identified as increased proteins, were higher in core-expressing cells than in control cells (Fig. 1C), whereas that of HSP60, which was identified as having a similar expression, was unchanged.

Up-regulation of Prohibitin by the Core Protein. Among the identified proteins, we focused on prohibitin, an up-regulated protein in mitochondria of core-expressing cells (Fig. 2A). Prohibitin is a mitochondrial protein associated with cell proliferation.[20] It also works as a chaperon of mitochondrial proteins.[21,22] We confirmed an increased prohibitin expression level in core-expressing cells

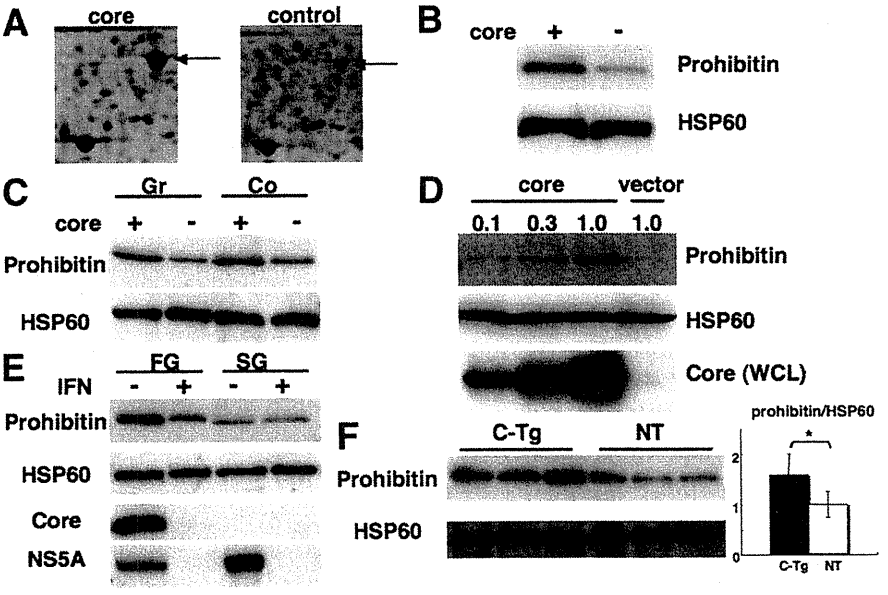

Fig. 2. Up-regulation of prohibitin in core-expressing cells. (A) Protein spot corresponding to prohibitin (arrow) in 2D-PAGE. (B) Purified mitochondria from core-expressing or control cells were subjected to SDS-PAGE and immunoblotted with anti-prohibitin or anti-HSP60 antibody. (C) Mitochondria were purified from growing (Gr) or confluent (Co) cells in 100-mm dishes and subjected to SDS-PAGE, then immunoblotted with an anti-prohibitin or anti-HSP60 antibody. (D) HepG2 cells in six-well plates were transfected with different amounts (μg) of core-expressing plasmid and mitochondrial proteins were analyzed by immunoblotting with anti-prohibitin or anti-HSP60 antibody. The expression levels of the core protein in whole-cell lysates (WCL) were also determined. (E) Cells harboring HCV replicon were untreated or treated with IFN and expression levels of prohibitin in mitochondria were determined. Expression of HCV core and NS5A proteins was also examined. FG, full-genomic replicon cells; SG, subgenomic replicon cells. (F) Expression levels of prohibitin in mitochondria were determined in liver tissues HCV core-gene transgenic and nontransgenic mice. Prohibitin/HSP60 expression levels were determined by densitometry. C-Tg, core-gene transgenic mouse; NT, nontransgenic littermate ($n = 3$) $^*P < 0.05$.

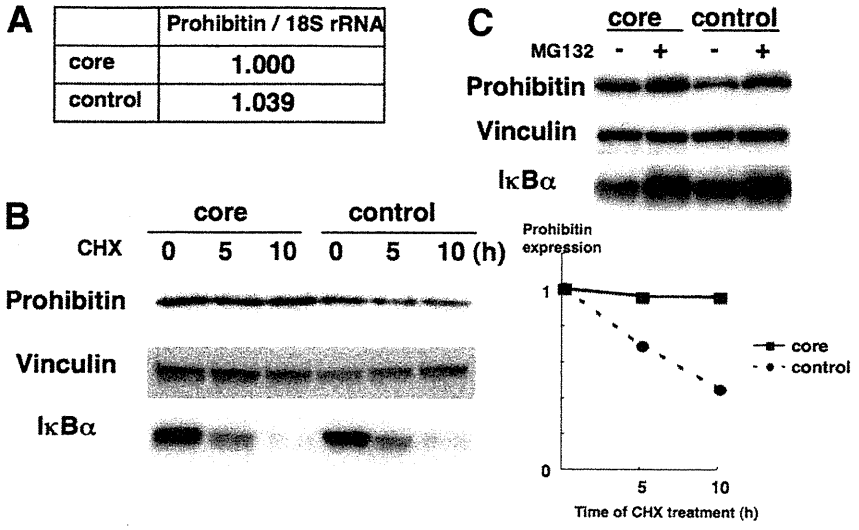

Fig. 3. Increased protein stability of prohibitin in core-expressing cells. (A) RNA was extracted from core-expressing and control cells, and the amount of specific mRNA was determined by real-time PCR with specific primers/probe against prohibitin. The amount of prohibitin mRNA was standardized by that of 18S ribosomal RNA (18S rRNA). (B) Cells were incubated with 100 ng/mL cycloheximide and harvested at the timepoints indicated above the lanes (numbers are hours of cycloheximide treatment). Whole-cell lysates were subjected to SDS-PAGE and immunoblotted with anti-prohibitin, anti-IκBα, or anti-vinculin (as an internal standard) antibody. The intensity of each band was measured by densitometry, and expression levels (prohibitin/vinculin) are shown in the right panel. (C) Cells were harvested after incubation with 20 μM MG132 for 8 hours and subjected to immunoblotting with anti-prohibitin, anti-IκBα, or anti-vinculin antibody.

by immunoblotting (Fig. 2B). Because prohibitin is associated with cell proliferation, it is possible that prohibitin expression changed according to the cell proliferative status. As shown in Fig. 2C, core-expressing cells had high prohibitin expression levels in the cells in both confluent growth and growing statuses compared with control cells. We also determined the expression levels in cells synchronized with aphidicolin followed by l-mimosine treatment and found an increased expression level in core-expressing cells (data not shown). To exclude the possibility that the increased prohibitin expression level is due to the expansion of limited cell clones, not specific to the core protein expression, we examined prohibitin expression in cells transiently expressing the core protein and found that prohibitin expression level increased dose-dependently in core-expressing cells (Fig. 2D). We also examined the prohibitin expression levels in Huh7 cells harboring full- or subgenomic HCV replicon. For this purpose, we used interferon (IFN)-treated replicon cells (cured cells) as a control. Core and nonstructural (NS)5A proteins were not detected after treatment of full-genomic replicon cells with IFN, suggesting a successful elimination of replicon. Prohibitin expression levels in cells with full-genomic replicon were increased compared with those in IFN-treated cured cells, whereas levels of prohibitin expression were low in subgenomic replicon cells regardless of IFN-treatment (Fig. 2E). In addition, prohibitin expression levels were also increased in livers of 3-month-old transgenic mice expressing the core protein compared with those in nontransgenic littermates (Fig. 2F).

We next sought to determine the mechanism of the increased steady-state level of prohibitin in core-expressing cells. To determine prohibitin messenger RNA (mRNA) expression, we performed a real-time polymerase chain reaction (PCR) using specific primers/probe. No difference in prohibitin mRNA was observed between core-expressing and control cells (Fig. 3A). We next determined the stability of prohibitin in these cells. By treating the cells with cycloheximide, the expression levels of prohibitin gradually decreased in control cells (Fig. 3B). On the other hand, in core-expressing cells prohibitin was hardly degraded by cycloheximide treatment for 10 hours, whereas IκBα was equally degraded in both cells. This result suggests that prohibitin was stabilized in the presence of the core protein. Because prohibitin has been shown to be degraded by proteasome,[23] we examined expression levels of prohibitin in the presence of proteasome inhibitor MG132. By treatment with MG132, prohibitin expression was increased to the similar level in core-expressing and control cells. These results suggest that the core protein may inhibit proteasomal degradation of prohibitin by some mechanism, including the prevention of degradation by interaction with the core protein. Then, core-expressing cells were lysed and subjected to immunoprecipitation with an anti-prohibitin antibody. As shown in Fig. 4, the core protein was coimmunoprecipitated with an anti-prohibitin antibody. To exclude a nonspecific interaction with the antibody or Sepharose beads, cells expressing a small amount of prohibitin by transfection with small interfering RNA (siRNA) against prohibitin were also examined. In these cells the amount of the coimmunoprecipitated core protein decreased. In addition, the core protein was not coimmunoprecipitated by control immunoglobulin G (IgG), indicating a specific interaction of prohibitin with the core protein. These results suggest that prohibitin expression increased in core-expressing cells owing to the increased stability presumably by interaction with the core protein.

Impaired Chaperon Function of Prohibitin in Core-Expressing Cells. We next examined the effect of

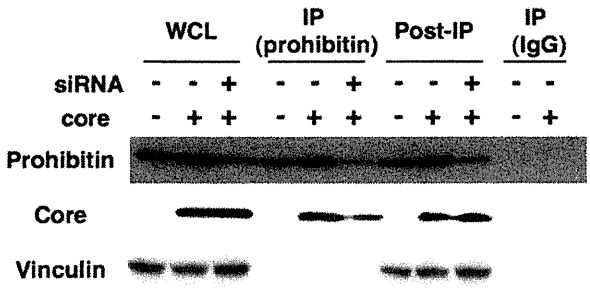

Fig. 4. Interaction of the core protein with prohibitin. Core-expressing and control cells were transfected with or without siRNA against the prohibitin gene, then harvested and lysed in NET-N buffer 3 days after transfection. Whole-cell lysates (WCL) were immunoprecipitated (IP) with an anti-prohibitin antibody or control IgG and immunoblotted with anti-prohibitin or anti-core antibody. Supernatants after the immunoprecipitation were harvested and similarly immunoblotted (Post-IP).

the interaction of prohibitin with the core protein on the function of prohibitin. Prohibitin works as a chaperon of mitochondrial proteins. Nijtmans et al.[21] demonstrated that prohibitin exerts a chaperon function particularly for the stabilization of mitochondrial DNA-encoded proteins. COX is a mitochondrial respiratory complex IV formed by 14 subunits, 10 of which are encoded by nuclear DNA and the rest by mitochondrial DNA.[24] We examined the interaction of prohibitin with subunit II of COX encoded by mitochondrial DNA. As shown in Fig. 5A, the level of COX II coimmunoprecipitated with an anti-prohibitin antibody was decreased in core-expressing cells, although the amount of immunoprecipitated prohibitin was higher than that in control cells. On the other hand, the subunit IV of COX encoded by nuclear DNA was similarly coimmunoprecipitated between core-expressing and control cells. When prohibitin expression was decreased by siRNA transfection, coimmunoprecipitation of COX subunits was similarly decreased with the amount of immunoprecipitation of prohibitin itself being low. We next determined expression levels of COX subunits in the mitochondria in these cells. Expression levels of mitochondrial DNA-encoded subunits I and II in core-expressing cells were decreased, whereas the levels of nuclear DNA-encoded subunits IV and VIb were similar to those in control cells. When transfected with prohibitin-siRNA, expression levels of all of the COX subunits examined were decreased in both core-expressing and control cells, suggesting that protein levels of these subunits are dependent on prohibitin (Fig. 5B, see Supporting Fig. 1 for densitometry). Similar data were observed when blots for COX II and IV were developed together in the same membrane (Supporting Fig. 2). We also determined COX activity in these cells and found that core-expressing cells had a significantly decreased COX activity (about 70% of that in control cells, Fig. 5C). These results suggest that interaction of prohibitin with the core protein is associated with an impaired function of prohibitin as a mitochondrial chaperon, which may trigger disordered assembly and function of mitochondrial respiratory complexes.

Discussion

In the present study we analyzed expression levels of mitochondrial proteins in HepG2 cells expressing the HCV core protein and identified a set of proteins with different expressions. Some of those proteins were related to the mitochondrial respiratory chain (Table 1). Because the core protein was shown to be associated with the induction of oxidative stress,[7-9] the core protein may modulate the expression and function of proteins forming mitochondrial respiratory complexes, which naturally

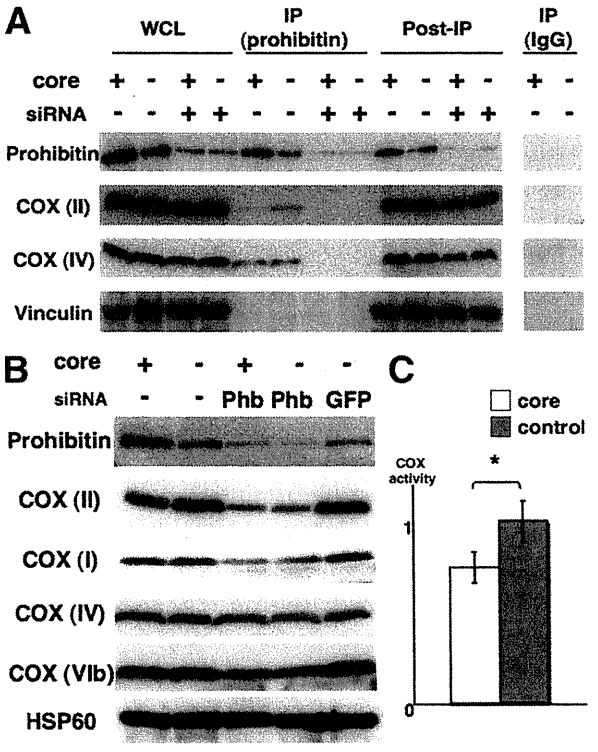

Fig. 5. Effects of core-prohibitin interaction on interaction/expression of COX subunit proteins and COX activity. (A) Whole-cell lysates (WCL) of core-expressing and control cells were subjected to immunoprecipitation with an anti-prohibitin antibody or control IgG, and the interaction of prohibitin with COX subunits was determined by immunoblotting of immunoprecipitated proteins (IP). Supernatants after the immunoprecipitation were harvested and similarly immunoblotted (Post-IP). (B) Cells were transfected with or without siRNA against the prohibitin (Phb) or GFP gene and harvested 3 days after transfection for purification of mitochondria. Purified mitochondria were subjected to SDS-PAGE and immunoblotted with several anti-COX subunits antibodies. The expression levels of HSP60 were also examined as an internal control. (C) COX activity was determined by measuring cytochrome c oxidation. The activity was normalized by taking the average rate of control cells as 1. Data shown are means ± SE ($n = 5$). *$P < 0.05$.

leads to ROS accumulation. In addition, MnSOD, which plays a key role in protecting cells from oxidative damage, was up-regulated in core-expressing cells, reflecting ROS increase in the cells. Several protein chaperons such as HSP70 and GrpE-like protein co-chaperon were also identified as up-regulated proteins. Because these proteins are known to be important in the mitochondrial protein-import mechanisms, the modulated expression of these proteins may be associated with the different expressions of the identified mitochondrial proteins.

Prohibitin, a mitochondrial protein chaperon, was identified as an up-regulated protein in core-expressing cells. Prohibitin is a ubiquitously expressed and highly conserved protein that was originally determined to play a predominant role in inhibiting cell-cycle progression and cellular proliferation by attenuating DNA synthesis.[20,25] Prohibitin is present in the nucleus and interacts with transcription factors that are important in cell cycle progression. In core-expressing cells used in this study, prohibitin was also detected in the nucleus and its expression level was also higher than that in control Hepswx cells or HepG2 cells (data not shown). The growth rate of core-expressing cells, however, was similar to that of control cells (data not shown). The physiological significance of the high expression level of prohibitin in the nucleus remains to be determined, but it may be related to enhanced apoptosis by Fas ligand, as shown by Ruggieri et al.,[16] because prohibitin interacts with E2F, Rb, and p53 and modulates the transcription activity of these factors and induces apoptosis.[26,27]

Mitochondrial prohibitin acts as a protein chaperon by stabilizing newly synthesized mitochondrial translation products through direct interaction.[21] We examined the interaction between prohibitin and mitochondrially encoded subunit II of COX and found a suppressed interaction between these proteins in core-expressing cells. In addition, there are several studies that showed the association of prohibitin with the assembly of mitochondrial respiratory complex I as well as complex IV (COX).[21,28] Complex I also consists of both nuclear- and mitochondrial-DNA-encoded subunits; therefore, it is probable that the assembly and function of complex I are impaired by the core protein. We attempted to examine the interaction of prohibitin with the mitochondrial DNA-encoded subunit of complex I, but commercially available antibodies against this subunit could not detect the protein itself by immunoblotting (data not shown). With respect to the complex I function, we found a decreased complex I activity in core-expressing cells (H. Miyoshi et al., manuscript in preparation). Other groups have also shown that complex I activity is decreased in the liver of transgenic mice harboring HCV core and envelope genes[9] as well as in cultured cells.[29] From these findings, the interaction between prohibitin and the core protein may impair the function of complex I as well as complex IV, leading to an increase in ROS production. In fact, the suppression of the prohibitin function is shown to result in an increased production of ROS,[30] a phenomenon observed in core-expressing cells used in this study (Miyoshi et al., in prep.) as well as in the liver of core-gene transgenic mice.[7,8] Interestingly, Berger and Yaffe[31] showed that loss of function of prohibitin leads to an altered mitochondrial morphology, that is, the loss of the normal reticular morphology and organized mitochondrial distribution. In hepatocytes from the core-gene transgenic mice, we observed a change in morphology of mitochondria, a disappearance of the double structure of mitochondrial membranes.[2] These changes in mitochondrial morphology are somewhat different, but the dysfunction of prohibitin may be responsible for the morphological abnormality of mitochondria observed in the core-gene transgenic mice.

We concluded that prohibitin overexpression is due to increased stability induced by the interaction with the core protein. In this study we showed that prohibitin might be degraded by proteasome, although we could not detect ubiquitinated forms of prohibitin. If the degradation is mediated by ubiquitin as reported,[23] it is possible that the interaction with the core protein interferes with ubiquitin-binding and protects prohibitin from degradation by proteasome. Some posttranslational protein modifications such as phosphorylation are other possible factors for the stabilization, because prohibitin can be serine-phosphorylated[32]; however, in our examination no serine/threonine/tyrosine phosphorylation of prohibitin was detected in core-expressing cells (data not shown). Thus far, there are no studies showing that prohibitin stabilization leads to a suppressed function as a mitochondrial chaperon. Therefore, this finding is novel and noteworthy because the prohibitin expression level has been considered to be proportional to the chaperon function. Prohibitin is highly expressed in several human tumors.[33,34] In addition, a 2D-PAGE of the hepatoma cell line HCC-M identified prohibitin as a positively regulated protein.[35] In these studies, the mechanism of prohibitin overexpression was not elucidated, but considering that prohibitin is associated with the inhibition of cell proliferation, the function of prohibitin is suppressed by stabilization by some molecules in the tumor, similar to the mechanism we suggest in the current study.

In addition to HepG2 cells constitutively expressing the core protein, increased prohibitin expression levels were also found in livers of core-gene transgenic mice.

The difference in expression levels between the transgenic mice and nontransgenic littermates, however, was a little bit smaller than that in the studies of HepG2 cells. This may be due to the low expression level of the core protein in the transgenic mice compared with that in core-expressing HepG2 cells because the expression level of prohibitin was proportionally increased to that of the core protein as shown in this study (Fig. 2D). Otherwise, there might be some *in vivo* mechanism for suppressing prohibitin expression in mice.

In this study, COX subunit IV as well as II were found to interact with prohibitin (Fig. 5A). Although there are no studies demonstrating that prohibitin also works as chaperon for nuclear DNA-encoded mitochondrial proteins as far as we investigated, knockdown of prohibitin expression by siRNA led to decreases in expression levels of both nuclear (COX IV, VIb) and mitochondrial (COX I, II) DNA-encoded subunits in mitochondria (Fig. 5B and Supporting Figs. 1 and 2). We showed that COX IV interacts with prohibitin (Fig. 4), suggesting that prohibitin also works for stable expression of nuclear DNA-encoded COX IV. Degrees of decrease in COX IV and VIb expression, however, were smaller than those in I and II. Prohibitin might contribute to stabilization of COX IV and VIb by mechanism(s) other than chaperon function. Steglich et al.[36] showed that prohibitin regulates protein degradation by the m-AAA protease in mitochondria. Recently, Da Cruz et al.[37] showed that SLP-2, a member of the stomatin gene family, interacts with prohibitin and regulates the expression of mitochondrial proteins such as COX IV and ND6 of complex I encoded by nuclear DNA by AAA proteases. In view of these findings, COX IV and VIb expression in mitochondria is dependent on prohibitin but other factors may also be involved in the attainment of stable expression of these subunits. The expression levels of COX II and IV in the whole-cell lysates were not so drastic among cell samples (Fig. 5A) compared to those in the mitochondria (Fig. 5B). The reason is not clear, but it is possible that redundant proteins such as improperly folded proteins by lack of chaperons were included in the whole-cell lysates.

In summary, we analyzed mitochondrial proteins in core-expressing HepG2 cells by proteomics analysis and identified prohibitin as an up-regulated protein. The dysfunction of prohibitin induced by the core protein may lead to ROS overproduction in the mitochondrion, which plays a key role in the pathogenesis of chronic hepatitis C. The restoration of prohibitin function might be a therapeutic option for correcting the dysregulated assembly and dysfunction of mitochondrial respiratory chain complexes.

Acknowledgment: We thank S. Shinzawa, M. Yahata, and S. Yoshizaki for technical assistance.

References

1. Suzuki R, Suzuki T, Ishii K, Matsuura Y, Miyamura T. Processing and functions of Hepatitis C virus proteins. Intervirology 1999;42:145-152.
2. Moriya K, Fujie H, Shintani Y, Yotsuyanagi H, Tsutsumi T, Ishibashi K, et al. The core protein of hepatitis C virus induces hepatocellular carcinoma in transgenic mice. Nat Med 1998;4:1065-1067.
3. Naas T, Ghorbani M, Alvarez-Maya I, Lapner M, Kothary R, De Repentigny Y, et al. Characterization of liver histopathology in a transgenic mouse model expressing genotype 1a hepatitis C virus core and envelope proteins 1 and 2. J Gen Virol 2005;86:2185-2196.
4. Machida K, Cheng KT, Lai CK, Jeng KS, Sung VM, Lai MM. Hepatitis C virus triggers mitochondrial permeability transition with production of reactive oxygen species, leading to DNA damage and STAT3 activation. J Virol 2006;80:7199-7207.
5. Suzuki R, Sakamoto S, Tsutsumi T, Rikimaru A, Tanaka K, Shimoike T, et al. Molecular determinants for subcellular localization of hepatitis C virus core protein. J Virol 2005;79:1271-1281.
6. Schwer B, Ren S, Pietschmann T, Kartenbeck J, Kaehlcke K, Bartenschlager R, et al. Targeting of hepatitis C virus core protein to mitochondria through a novel C-terminal localization motif. J Virol 2004;78:7958-7968.
7. Moriya K, Nakagawa K, Santa T, Shintani Y, Fujie H, Miyoshi H, et al. Oxidative stress in the absence of inflammation in a mouse model for hepatitis C virus-associated hepatocarcinogenesis. Cancer Res 2001;61:4365-4370.
8. Okuda M, Li K, Beard MR, Showalter LA, Scholle F, Lemon SM, et al. Mitochondrial injury, oxidative stress, and antioxidant gene expression are induced by hepatitis C virus core protein. Gastroenterology 2002;122:366-375.
9. Korenaga M, Wang T, Li Y, Showalter LA, Chan T, Sun J, et al. Hepatitis C virus core protein inhibits mitochondrial electron transport and increases reactive oxygen species (ROS) production. J Biol Chem 2005;280:37481-37488.
10. Diamond DL, Jacobs JM, Paeper B, Proll SC, Gritsenko MA, Carithers RL Jr, et al. Proteomic profiling of human liver biopsies: hepatitis C virus-induced fibrosis and mitochondrial dysfunction. HEPATOLOGY 2007;46:649-657.
11. Moriya K, Yotsuyanagi H, Shintani Y, Fujie H, Ishibashi K, Matsuura Y, et al. Hepatitis C virus core protein induces hepatic steatosis in transgenic mice. J Gen Virol 1997;78(Pt 7):1527-1531.
12. Moriya K, Todoroki T, Tsutsumi T, Fujie H, Shintani Y, Miyoshi H, et al. Increase in the concentration of carbon 18 monounsaturated fatty acids in the liver with hepatitis C: analysis in transgenic mice and humans. Biochem Biophys Res Commun 2001;281:1207-1212.
13. Fujie H, Yotsuyanagi H, Moriya K, Shintani Y, Tsutsumi T, Takayama T, et al. Steatosis and intrahepatic hepatitis C virus in chronic hepatitis. J Med Virol 1999;59:141-145.
14. Cho WC. Contribution of oncoproteomics to cancer biomarker discovery. Mol Cancer 2007;6:25.
15. Lescuyer P, Strub JM, Luche S, Diemer H, Martinez P, Van Dorsselaer A, et al. Progress in the definition of a reference human mitochondrial proteome. Proteomics 2003;3:157-167.
16. Ruggieri A, Harada T, Matsuura Y, Miyamura T. Sensitization to Fas-mediated apoptosis by hepatitis C virus core protein. Virology 1997;229:68-76.
17. Okado-Matsumoto A, Fridovich I. Subcellular distribution of superoxide dismutases (SOD) in rat liver: Cu,Zn-SOD in mitochondria. J Biol Chem 2001;276:38388-38393.
18. Murakami K, Ishii K, Ishihara Y, Yoshizaki S, Tanaka K, Gotoh Y, et al. Production of infectious hepatitis C virus particles in three-dimensional cultures of the cell line carrying the genome-length dicistronic viral RNA of genotype 1b. Virology 2006;351:381-392.

19. Shevchenko A, Wilm M, Vorm O, Mann M. Mass spectrometric sequencing of proteins silver-stained polyacrylamide gels. Anal Chem 1996;68: 850-858.
20. Mishra S, Murphy LC, Murphy LJ. The prohibitins: emerging roles in diverse functions. J Cell Mol Med 2006;10:353-363.
21. Nijtmans LG, de Jong L, Artal Sanz M, Coates PJ, Berden JA, Back JW, et al. Prohibitins act as a membrane-bound chaperone for the stabilization of mitochondrial proteins. EMBO J 2000;19:2444-2451.
22. Back JW, Sanz MA, De Jong L, De Koning LJ, Nijtmans LG, De Koster CG, et al. A structure for the yeast prohibitin complex: structure prediction and evidence from chemical crosslinking and mass spectrometry. Protein Sci 2002;11:2471-2478.
23. Thompson WE, Ramalho-Santos J, Sutovsky P. Ubiquitination of prohibitin in mammalian sperm mitochondria: possible roles in the regulation of mitochondrial inheritance and sperm quality control. Biol Reprod 2003; 69:254-260.
24. Fontanesi F, Soto IC, Horn D, Barrientos A. Assembly of mitochondrial cytochrome c-oxidase, a complicated and highly regulated cellular process. Am J Physiol Cell Physiol 2006;291:C1129-C1147.
25. Mishra S, Murphy LC, Nyomba BL, Murphy LJ. Prohibitin: a potential target for new therapeutics. Trends Mol Med 2005;11:192-197.
26. Fusaro G, Dasgupta P, Rastogi S, Joshi B, Chellappan S. Prohibitin induces the transcriptional activity of p53 and is exported from the nucleus upon apoptotic signaling. J Biol Chem 2003;278:47853-47861.
27. Joshi B, Ko D, Ordonez-Ercan D, Chellappan SP. A putative coiled-coil domain of prohibitin is sufficient to repress E2F1-mediated transcription and induce apoptosis. Biochem Biophys Res Commun 2003;312:459-466.
28. Bourges I, Ramus C, Mousson de Camaret B, Beugnot R, Remacle C, Cardol P, et al. Structural organization of mitochondrial human complex I: role of the ND4 and ND5 mitochondria-encoded subunits and interaction with prohibitin. Biochem J 2004;383:491-499.
29. Piccoli C, Scrima R, Quarato G, D'Aprile A, Ripoli M, Lecce L, et al. Hepatitis C virus protein expression causes calcium-mediated mitochondrial bioenergetic dysfunction and nitro-oxidative stress. HEPATOLOGY 2007;46:58-65.
30. Theiss AL, Idell RD, Srinivasan S, Klapproth JM, Jones DP, Merlin D, et al. Prohibitin protects against oxidative stress in intestinal epithelial cells. FASEB J 2007;21:197-206.
31. Berger KH, Yaffe MP. Prohibitin family members interact genetically with mitochondrial inheritance components in Saccharomyces cerevisiae. Mol Cell Biol 1998;18:4043-4052.
32. Ross JA, Nagy ZS, Kirken RA. The PHB1/2 phosphocomplex is required for mitochondrial homeostasis and survival of human T cells. J Biol Chem 2008;283:4699-4713.
33. Coates PJ, Nenutil R, McGregor A, Picksley SM, Crouch DH, Hall PA, et al. Mammalian prohibitin proteins respond to mitochondrial stress and decrease during cellular senescence. Exp Cell Res 2001;265:262-273.
34. Asamoto M, Cohen SM. Prohibitin gene is overexpressed but not mutated in rat bladder carcinomas and cell lines. Cancer Lett 1994;83:201-207.
35. Seow TK, Ong SE, Liang RC, Ren EC, Chan L, Ou K, et al. Two-dimensional electrophoresis map of the human hepatocellular carcinoma cell line, HCC-M, and identification of the separated proteins by mass spectrometry. Electrophoresis 2000;21:1787-1813.
36. Steglich G, Neupert W, Langer T. Prohibitins regulate membrane protein degradation by the m-AAA protease in mitochondria. Mol Cell Biol 1999; 19:3435-3442.
37. Da Cruz S, Parone PA, Gonzalo P, Bienvenut WV, Tondera D, Jourdain A, et al. SLP-2 interacts with prohibitins in the mitochondrial inner membrane and contributes to their stability. Biochim Biophys Acta 2008;1783: 904-911.

[a]*Avon Orthopaedic Centre, Bristol, UK*
[b]*Department of Microbiology, Southmead Hospital, Bristol, UK*
E-mail address: alannapentlow@doctors.org.uk

Available online 28 August 2009

* Corresponding author. Address: Department of Microbiology, Southmead Hospital, Southmead Road, Bristol BS10 5NB, UK. Tel.: +44 797 618 8454; fax: +44 117 959 5901.

doi:10.1016/j.jhin.2009.06.014

Evaluation of the efficacy of a low temperature steam and formaldehyde steriliser by using biological indicators

Madam,

Medical instruments, such as rigid and flexible operative endoscopes, including accessories, must be sterilised using properly validated processes.[1] Laparoscopic, urological and arthroscopic telescopes and their accessories are now largely heat tolerant and may be autoclaved, but nevertheless some are heat labile, as are all flexible fibreoptic or video endscopes. These are best sterilised using ethylene oxide (EO), gas plasma or low temperature steam and formaldehyde (LTSF).[1] LTSF sterilisers are used in European countries, and their usefulness and safety for sterilisation of heat-labile materials has been reported.[2–4] In this study, we evaluated the efficacy of an LTSF steriliser, Matachana 130LF (Matachana, Barcelona, Spain) by using biological indicators (BIs).

The LTSF steriliser Matachana 130LF, which fulfils all the requirements of the forthcoming European Norm for LTSF sterilisers (EN 14180, EN 61326-1, EN 60204-1, EN 61010-1 and EN 61010-2-042), was used. The sterilisation cycle consists of six phases: pre-vacuum, pre-pulses of steam, formaldehyde feed, sterilisation, washing pulses, and air pulses. Three BIs including *Geobacillus stearothermophilus* ATCC 7953 were used to assess sterilisation: a filter paper containing 2.3×10^6 spores (Statens Serum Institute, Copenhagen, Denmark) (SSI BI), a filter paper containing 1.7×10^6 spores (SGM, Bozeman, MT) (SGM BI) and a filter paper containing 1.9×10^5 spores (Simicon, Munich, Germany). A BI was placed into a process challenge device (PCD) which was made by Udono Co., Inc. (Tokyo, Japan) based on a standard of EN 14180 and was packed in a sterilisation bag (Sengewald, Rohrdorf, Germany) attached to the chemical indicators for LTSF before sterilisation. For the sterilisation temperature of 60 °C, the times of sterilisation processes were 5, 10, 15, 20, and 30 min. After the sterilisation process was completed, the filter paper was removed from the PCD and placed in a test tube with 10 mL tryptone soya broth (CM0129, Oxoid, Basingstoke, UK). The filter paper was cultured at 56 °C for 7 days. Positive results were inferred when turbidity was seen with the naked eye. Gram-positive bacilli were confirmed by Gram stain and were identified by using the Vitek 1 system (Sysmex-bioMérieux, Tokyo, Japan). An unsterilised BI was used as the positive control for each experiment. All experiments were repeated four times.

A total of 56 BIs were cultured and results are shown in Table I. Although the cultures of the SSI BIs following 5, 10, and 15 min sterilisation cycles were positive, the culture of the remaining BIs yielded no growth. Bacterial growth was present in all the positive control cultures and it confirmed that the positive sample was *G. stearothermophilus*. The number of spores contained in the SSI BI (2.3×10^6 spores) is 1.4 and 12 times that of the SGM BI (1.7×10^6 spores) and the Simicon BI (1.9×10^5 spores), respectively. Using *G. stearothermophilus* ATCC 7953 at more than 10^5 spores as a BI for LTSF is recommended with the standard (ISO 11138-5 and EN 866-5). Hence, when the sterilisation process used a programme temperature of 60 °C it could be suggested that the sterilisation process would need to be longer than 20 min. Moreover, no growth was seen in cultures for reference strains, clinical and environmental isolates,

Table I Sterilisation time at 60 °C and growth of biological indicators after low temperature steam and formaldehyde sterilisation

Sterilisation (min)	Biological indicators (spores)		
	SSI[a] (2.3×10^6)	SGM (1.7×10^6)	Simicon (1.9×10^5)
5	+ (3)	–	–
10	+ (1)	–	–
15	+ (1)	–	–
20	–	–	–
30	–	–	NT

+, culture positive (the number of positive samples); –, culture negative; NT, not tested.
[a] Statens Serum Institute.

such as *Escherichia coli* ATCC 25922, *Pseudomonas aeruginosa* ATCC 27853, *Staphylococcus aureus* ATCC 25923, *Streptococcus pneumoniae* ATCC 6305, *Haemophilus influenzae* ATCC 35056, meticillin-resistant *S. aureus* (clinical isolate), extended spectrum β-lactamase-producing *E. coli* (clinical isolate), metallo β-lactamase-producing *P. aeruginosa* (clinical isolate), multidrug-resistant *P. aeruginosa* (clinical isolate), *Pseudomonas putida* (environmental isolate), *Acinetobacter* spp. (environmental isolate), Candida albicans (environmental isolate).

Some medical equipment, such as endoscopes, may be used more than once a day. This study demonstrated that sterilisation temperature of less than 60 °C requires a cycle time of more than 20 min. Although an EO gas steriliser requires at least 24 h, the LTSF steriliser requires only 3.5 h.[4] Additionally, the LTSF steriliser has been reported as an adequate and reliable method for flexible endoscopes.[4,5] Furthermore, the formaldehyde residues after LTSF sterilisation were all below the value as indicated by the EN 14180 in the present study (data not shown). In conclusion, the benefits of LTSF sterilisation are efficacy, short cycle time, and safety.

Conflict of interest statement
None declared.

Funding sources
None.

References

1. Ayliffe G. Decontamination of minimally invasive surgical endoscopes and accessories. *J Hosp Infect* 2000;**45**: 263–277.
2. Gibson GL. Processing heat-sensitive instruments and materials by low-temperature steam and formaldehyde. *J Hosp Infect* 1980;**1**:95–101.
3. Robertshaw RG. Low temperature steam and formaldehyde sterilization. *J Hosp Infect* 1983;**4**:305–314.
4. Kanemitsu K, Kunishima H, Imasaka T, *et al*. Evaluation of a low-temperature steam and formaldehyde sterilizer. *J Hosp Infect* 2003;**55**:47–52.
5. Adler S, Scherrer M, Daschner FD. Costs of low-temperature plasma sterilization compared with other sterilization methods. *J Hosp Infect* 1998;**40**:125–134.

R. Saito[a,*]
Y. Uetera[b]
Y. Saito[b]
N. Okamura[c]
K. Moriya[a]
K. Koike[a]

[a]*Department of Infection Control and Prevention, University of Tokyo Hospital, Tokyo, Japan*
[b]*Department of Hospital Environment, Surgical Center, University of Tokyo Hospital, Tokyo, Japan*
[c]*Department of Microbiology and Immunology, Graduate School of Health Sciences, Tokyo Medical and Dental University, Tokyo, Japan*
E-mail address: saito-lab@umin.ac.jp

Available online 22 August 2009

* Corresponding author. Address: Department of Infection Control and Prevention, University of Tokyo Hospital, 7-3-1 Hongo, Bunkyo-ku, Tokyo 113-8655, Japan. Tel.: +81 3 3815 5411x35028; fax: +81 3 5689 0495.

doi:10.1016/j.jhin.2009.06.018

Combined effect of copper and silver against *Pseudomonas aeruginosa*

Madam,

Infection from *Pseudomonas aeruginosa* is an increasing cause for concern in the healthcare environment and it is associated with chronic lung infections, particularly in patients with cystic fibrosis. The Health Protection Agency has reported a 20% increase in cases of *P. aeruginosa* nosocomial infections since 2003. *P. aeruginosa* exhibits multiple drug resistance and it is feared that a total drug resistance will eventually emerge.[1]

Copper and silver both have an antimicrobial effect against a range of pathogens, with a $\geq$2.5 $\log_{10}$ reduction observed against *Clostridium difficile* after 3 h exposure to copper surfaces and a 3 $\log_{10}$ cfu/mL increased reduction in meticillin-resistant *Staphylococcus aureus* from silver-impregnated wound dressings compared to controls.[2,3]

There is limited published research on the antimicrobial synergy between copper and silver; therefore, an investigation was conducted to assess their combined antimicrobial effect against *P. aeruginosa*.

The micro-organism tested was *Pseudomonas aeruginosa* ATCC 10145, grown in nutrient broth (CM0001) and cultured on nutrient agar (CM0003, Oxoid Ltd, Basingstoke, UK). Minimum inhibitory

nature genetics

Genome-wide association of *IL28B* with response to pegylated interferon-α and ribavirin therapy for chronic hepatitis C

Yasuhito Tanaka[1,18], Nao Nishida[2,18], Masaya Sugiyama[1], Masayuki Kurosaki[3], Kentaro Matsuura[1], Naoya Sakamoto[4], Mina Nakagawa[4], Masaaki Korenaga[5], Keisuke Hino[5], Shuhei Hige[6], Yoshito Ito[7], Eiji Mita[8], Eiji Tanaka[9], Satoshi Mochida[10], Yoshikazu Murawaki[11], Masao Honda[12], Akito Sakai[12], Yoichi Hiasa[13], Shuhei Nishiguchi[14], Asako Koike[15], Isao Sakaida[16], Masatoshi Imamura[17], Kiyoaki Ito[17], Koji Yano[17], Naohiko Masaki[17], Fuminaka Sugauchi[1], Namiki Izumi[3], Katsushi Tokunaga[2] & Masashi Mizokami[1,17]

The recommended treatment for patients with chronic hepatitis C, pegylated interferon-α (PEG-IFN-α) plus ribavirin (RBV), does not provide sustained virologic response (SVR) in all patients. We report a genome-wide association study (GWAS) to null virological response (NVR) in the treatment of patients with hepatitis C virus (HCV) genotype 1 within a Japanese population. We found two SNPs near the gene *IL28B* on chromosome 19 to be strongly associated with NVR (rs12980275, $P = 1.93 \times 10^{-13}$, and rs8099917, 3.11×10^{-15}). We replicated these associations in an independent cohort (combined *P* values, 2.84×10^{-27} (OR = 17.7; 95% CI = 10.0–31.3) and 2.68×10^{-32} (OR = 27.1; 95% CI = 14.6–50.3), respectively). Compared to NVR, these SNPs were also associated with SVR (rs12980275, $P = 3.99 \times 10^{-24}$, and rs8099917, $P = 1.11 \times 10^{-27}$). In further fine mapping of the region, seven SNPs (rs8105790, rs11881222, rs8103142, rs28416813, rs4803219, rs8099917 and rs7248668) located in the *IL28B* region showed the most significant associations ($P = 5.52 \times 10^{-28}$–2.68×10^{-32}; OR = 22.3–27.1). Real-time quantitative PCR assays in peripheral blood mononuclear cells showed lower *IL28B* expression levels in individuals carrying the minor alleles ($P = 0.015$).

Hepatitis C is a global health problem that affects a significant proportion of the world's population. The World Health Organization estimated that in 1999, there were 170 million HCV carriers worldwide, with 3–4 million new cases appearing each year. HCV infection affects more than 4 million people in the United States, where it represents the leading cause of cirrhosis and hepatocellular carcinoma as well as the leading cause of liver transplantation[1]. The American Gastroenterological Association estimated that drugs are the largest direct costs of hepatitis C[1].

The most effective current standard of care in patients with chronic hepatitis C, a combination of PEG-IFN-α with ribavirin, does not produce SVR in all patients treated. Large-scale studies on 48-week-long PEG-IFN-α/RBV treatment in the United States and Europe showed that 42–52% of patients with HCV genotype 1 achieved SVR[2–4], and similar results were found in Japan. However, older patients (greater than 50 years of age) had a significantly lower rate of SVR due to poor adherence resulting from adverse events and laboratory-detectable abnormalities such as neutropenia and thrombocytopenia[5,6]. Specifically, various well-described side effects (such as a flu-like syndrome, hematologic abnormalities and adverse neuropsychiatric events) often necessitate dose reduction, and 10–14% of patients require premature withdrawal from interferon-based therapy[7]. To avoid these side effects in patients who will not be helped by the treatment, as well as to reduce the substantial cost of PEG-IFN-α/RBV treatment, it would be useful to be able to predict an individual's response before or early in treatment. Several viral factors, such as genotype 1, high baseline viral load, viral

[1]Department of Clinical Molecular Informative Medicine, Nagoya City University Graduate School of Medical Sciences, Nagoya, Japan. [2]Department of Human Genetics, Graduate School of Medicine, The University of Tokyo, Tokyo, Japan. [3]Division of Gastroenterology and Hepatology, Musashino Red Cross Hospital, Tokyo, Japan. [4]Department of Gastroenterology and Hepatology, Tokyo Medical and Dental University, Tokyo, Japan. [5]Division of Hepatology and Pancreatology, Kawasaki Medical College, 577 Matsushima, Kurashiki, Japan. [6]Department of Internal Medicine, Hokkaido University Graduate School of Medicine, Sapporo, Japan. [7]Molecular Gastroenterology and Hepatology, Kyoto Prefectural University of Medicine, Kyoto, Japan. [8]National Hospital Organization Osaka National Hospital, Osaka, Japan. [9]Department of Medicine, Shinshu University School of Medicine, Matsumoto, Japan. [10]Division of Gastroenterology and Hepatology, Internal Medicine, Saitama Medical University, Saitama, Japan. [11]Second department of Internal Medicine, Faculty of Medicine, Tottori University, Yonago, Japan. [12]Department of Gastroenterology, Kanazawa University Graduate School of Medicine, Kanazawa, Japan. [13]Department of Gastroenterology and Metabology, Ehime University Graduate School of Medicine, Ehime, Japan. [14]Department of Internal Medicine, Hyogo College of Medicine, Nishinomiya, Japan. [15]Central Research Laboratory, Hitachi Ltd., Kokubunji, Japan. [16]Gastroenterology and Hepatology, Yamaguchi University Graduate School of Medicine, Yamaguchi, Japan. [17]Research Center for Hepatitis and Immunology, International Medical Center of Japan Konodai Hospital, Ichikawa, Japan. [18]These authors contributed equally to this work. Correspondence should be addressed to M.M. (mmizokami@imcjk2.hosp.go.jp).

Received 29 June; accepted 21 August; published online 13 September 2009; doi:10.1038/ng.449

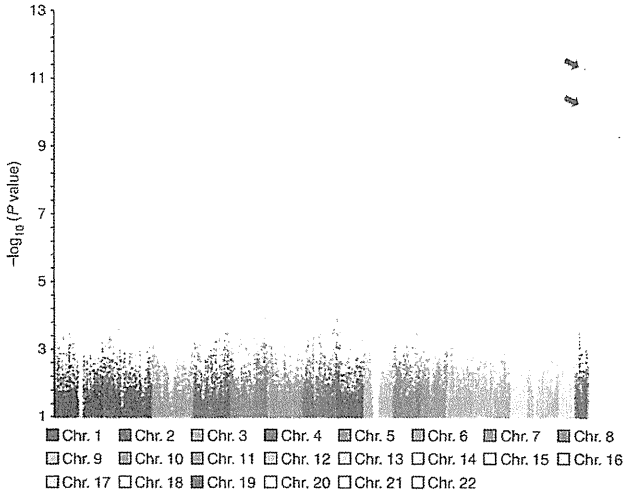

Figure 1 Genome-wide association results with PEG-IFN-α/RBV treatment in 142 Japanese patients with HCV (78 NVR and 64 VR samples). *P* values were calculated by using a χ^2 test for allele frequencies. The dots with arrows for chromosome 19 denote SNPs that showed significant genome-wide associations ($P < 8.05 \times 10^{-8}$) with response to PEG-IFN-α/RBV treatment.

kinetics during treatment, and amino acid pattern in the interferon sensitivity–determining region, have been reported to be significantly associated with the treatment outcome in a number of independent studies[8–10]. Studies have also provided strong evidence that ~20% of patients with HCV genotype 1 and 5% of patients with genotype 2 or 3 have a null response to PEG-IFN-α/RBV. No definite predictor of this resistance is currently available that make it possible to bypass the initial 12–24 weeks' treatment before deciding whether treatment should be continued. If a reliable predictor of non-response were identified for use in patients before treatment initiation, then an estimated 20%, including those who have little or no chance to achieve SVR, could be spared the side effects and cost of treatment.

Host factors, including age, sex, race, liver fibrosis and obesity, have also been reported to be associated with PEG-IFN-α/RBV therapy outcome[11,12]. However, little is known about the host genetic factors that might be associated with the response to therapy: thus far only a few candidate genes, including those encoding type I interferon receptor-1 (*IFNAR1*) and mitogen-activated protein kinase–activated protein kinase 3 (*MAPKAPK3*), have been reported to be associated with treatment response[13,14]. We describe here a GWAS for response to PEG-IFN-α/RBV treatment.

We conducted this GWAS to identify host genes associated with response to PEG-IFN-α/RBV treatment in 154 Japanese patients with HCV genotype 1 (82 with NVR and 72 with virologic response (VR), based on the selection criteria as described in Online Methods). We used the Affymetrix SNP 6.0 genome-wide SNP typing array for 900,000 SNPs. A total of 621,220 SNPs met the following criteria: (i) SNP call rate ≥95%, (ii) minor allele frequency (MAF) ≥1% and (iii) deviation from Hardy-Weinberg equilibrium (HWE) $P \geq 0.001$ in VR samples. After excluding 4 NVR and 8 VR samples that showed quality control (QC) call rates of <95%, 78 NVR and 64 VR samples were included in the association analysis. **Figure 1** shows a genome-wide view of the single-point association data based on allele frequencies. Two SNPs located close to *IL28B* on chromosome 19 showed strong associations, with a minor allele dominant model (rs12980275, $P = 1.93 \times 10^{-13}$, and rs8099917, $P = 3.11 \times 10^{-15}$, respectively), with NVR to PEG-IFN-α/RBV treatment (**Table 1**). The rs8099917 lies between *IL28B* and *IL28A*, ~8 kb downstream from *IL28B* and ~16 kb upstream from *IL28A*. These associations reached genome-wide levels of significance for both SNPs in this initial GWAS cohort (Bonferroni criterion $P < 8.05 \times 10^{-8}$ (0.05/621,220)). The frequencies of minor allele–positive patients were much higher in the NVR group than in the VR group for both SNPs (74.3% in NVR, 12.5% in VR for rs12980275; 75.6% in NVR, 9.4% in VR for rs8099917). Notably, individuals homozygous for the minor allele were observed only in the NVR group. The VR group, as compared to the NVR group, showed genotype frequencies closer to those in the healthy Japanese population[15], yet the minor allele frequencies were slightly higher in the transient virologic response (TVR) group (23.1%, 15.4%) than in the SVR group (9.8%, 7.8%) (**Table 1**). We applied the Cochrane-Armitage test on all the SNPs and found a genetic inflation factor, λ, of 1.029 for the GWAS stage (**Supplementary Fig. 1**). We also carried out principal component analysis in 142 samples for the GWAS stage together with the HapMap samples (CEU, YRI, CHB and JPT) (**Supplementary Fig. 2**); this suggested that the effect of population stratification was negligible.

Table 1 Significant association of two SNPs (rs12980275 and rs8099917) with response to PEG-IFN-α/RBV treatment

					Null responder (NVR[a], *n* = 128)			Responder (VR[a], *n* = 186)			Responder (SVR[a], *n* = 140)			NVR vs. VR		NVR vs. SVR	
dbSNP rsID	Nearest gene	MAF[b] (allele)	Allele (1/2)	Stage	11	12	22	11	12	22	11	12	22	OR (95% CI)[c]	*P* value[d]	OR (95% CI)[c]	*P* value[d]
rs12980275	*IL28B*	0.15 (G)	A/G	GWAS	20 (25.6)	54 (69.2)	4 (5.1)	56 (87.5)	8 (12.5)	0 (0.0)	46 (90.2)	5 (9.8)	0 (0.0)	20.3 (8.3–49.9)	1.93×10^{-13}	26.7 (9.3–76.5)	7.41×10^{-13}
				Replication	10 (20.0)	37 (74.0)	3 (6.0)	101 (82.8)	21 (17.2)	0 (0.0)	73 (82.0)	16 (18.0)	0 (0.0)	19.2 (8.3–44.4)	5.46×10^{-15}	18.3 (7.6–44.0)	8.37×10^{-13}
				Combined	30 (23.4)	91 (71.1)	7 (5.5)	157 (84.4)	29 (15.6)	0 (0.0)	119 (85.0)	21 (15.0)	0 (0.0)	17.7 (10.0–31.3)	2.84×10^{-27}	18.5 (10.0–34.4)	3.99×10^{-24}
rs8099917	*IL28B*	0.12 (G)	T/G	GWAS	19 (24.4)	56 (71.8)	3 (3.8)	58 (90.6)	6 (9.4)	0 (0.0)	47 (92.2)	4 (7.8)	0 (0.0)	30.0 (11.2–80.5)	3.11×10^{-15}	36.5 (11.6–114.6)	5.00×10^{-14}
				Replication	11 (22.0)	37 (74.0)	2 (4.0)	108 (88.5)	14 (11.5)	0 (0.0)	78 (87.6)	11 (12.4)	0 (0.0)	27.4 (11.5–65.3)	9.47×10^{-18}	25.1 (10.0–63.1)	1.00×10^{-14}
				Combined	30 (23.4)	93 (72.7)	5 (3.9)	166 (89.2)	20 (10.8)	0 (0.0)	125 (89.3)	15 (10.7)	0 (0.0)	27.1 (14.6–50.3)	2.68×10^{-32}	27.2 (13.9–53.4)	1.11×10^{-27}

[a]NVR, null virologic response; VR, virologic response; SVR, sustained virologic response. The 186 VRs consisted of 46 transient virologic response (TVRs) and 140 SVRs. [b]Minor allele frequency and minor allele in 184 healthy Japanese individuals[15]. The MAF of the SNPs in SVR is similar to that of TVR group, whereas that of NVR is much higher (76.6%). [c]Odds ratio for the minor allele in a dominant model. [d]*P* value by χ^2 test for the minor allele dominant model.

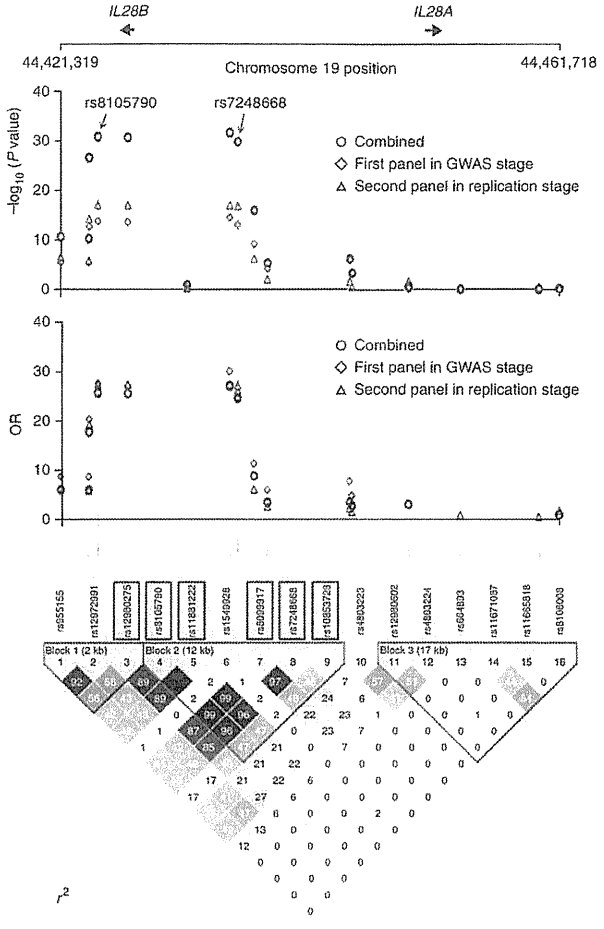

Figure 2 Genomic structure, *P* value and OR plots in association analysis and LD map around *IL28B* and *IL28A* (chr.19, nucleotide positions 44421319–44461718; build 35). *P* values by the χ^2 test for minor allele dominant effect model are shown for the first panel of 142 samples in the GWAS stage, the second panel of 172 samples in the replication stage, and the combined analysis. Below are estimates of pairwise r^2 for 16 SNPs selected in the replication study using a total of 314 Japanese patients with HCV treated with PEG-IFN-α/RBV. Boxes indicate the significantly associated SNPs with response to PEG-IFN-α/RBV treatment both in the GWAS stage and in the replication stage. Dotted lines indicate the region with the strongest associations from the positions of rs8105790 to rs7248668.

We analyzed the region of ~40 kb (chr. 19, nucleotide positions 44421319–44461718; build 35) containing the significantly associated SNPs (rs12980275 and rs8099917) using Haploview software for linkage disequilibrium (LD) and haplotype structure based on the HapMap data for individuals of Japanese ancestry. The LD blocks were analyzed using the four-gamete rule, and four blocks were observed (**Supplementary Fig. 3**). We selected 16 SNPs for both replication study and high-density association mapping, including tagging SNPs estimated on the basis of the haplotype blocks, one SNP located within *IL28B* (rs11881222) and the significantly associated SNPs from the GWAS stage (rs12980275 and rs8099917) (**Supplementary Table 1**).

To validate the results of the GWAS stage, 16 SNPs selected for the replication stage, including the original SNPs, were genotyped using the DigiTag2 assay in an independent set of 172 Japanese patients with HCV treated with PEG-IFN-α/RBV treatment (50 NVR and 122 VR samples), together with the first panel of 142 samples analyzed in the GWAS stage (**Supplementary Table 1**). The associations of the original SNPs were replicated in the replication cohort of 172 patients ($P = 5.46 \times 10^{-15}$, OR = 19.2 for rs12980275; $P = 9.47 \times 10^{-18}$, OR = 27.4 for rs8099917; **Table 1**). The combined *P* values for both stages reached 2.84×10^{-27} (OR = 17.7; 95% CI = 10.0–31.3) and 2.68×10^{-32} (OR = 27.1; 95% CI = 14.6–50.3), respectively (**Table 1**). Notably, when we compared the SVR ($n = 140$) with the NVR group ($n = 128$), the original two SNPs (rs12980275 and rs8099917) again showed strong associations: both *P* values and ORs were similar to those observed in the comparison between VR and NVR, and the combined *P* values for both stages reached 3.99×10^{-24} (OR = 18.5; 95% CI = 10.0–34.4) and 1.11×10^{-27} (OR = 27.2; 95% CI = 13.9–53.4), respectively (**Table 1**). Comparing SVR ($n = 140$) versus NVR plus TVR ($n = 174$), we again found that these SNPs were significantly associated ($P = 1.71 \times 10^{-16}$, OR = 8.8; 95% CI 5.1–15.4 for rs12980275; $P = 1.18 \times 10^{-18}$, OR = 12.1; 95% CI 6.5–22.4 for rs8099917, **Supplementary Table 2**), suggesting that these SNPs would predict NVR as well as SVR before PEG-IFN-α/RBV therapy.

Among the newly analyzed SNPs in the replication study, six (rs12980275, rs8105790, rs11881222, rs8099917, rs7248668 and rs10853728) showed significant associations both in the GWAS stage ($P < 8.05 \times 10^{-8}$) and in the replication stage ($P < 0.0031$ (0.05/16)) after Bonferroni correction. These SNPs are located within a 15.7-kb region that includes *IL28B* (**Fig. 2** and **Supplementary Table 1**). In particular, the strongest associations with NVR were observed for four SNPs, rs8105790, rs11881222, rs8099917 and rs7248668, that are located in the downstream flanking region, the third intron and the upstream flanking region of *IL28B*. The combined *P* values for these polymorphisms were 1.98×10^{-31} (OR = 25.7; 95% CI = 13.9–47.6), 2.84×10^{-31} (OR = 25.6; 95% CI = 13.8–47.3), 2.68×10^{-32} (OR = 27.1; 95% CI = 14.6–50.3) and 1.84×10^{-30} (OR = 24.7; 95% CI = 13.3–45.8), respectively (**Supplementary Table 1**). We then sequenced this region to identify further variants and found three SNPs (rs8103142, rs28416813 and rs4803219) located in the third exon, the first intron and the upstream flanking region of *IL28B*, and a few infrequent variations. These SNPs also showed strong associations in the combined dataset of 128 NVR and 186 VR samples ($P = 1.40 \times 10^{-29}$, OR = 26.6 for rs8103142; $P = 5.52 \times 10^{-28}$, OR = 22.3 for rs28416813; $P = 2.45 \times 10^{-29}$, OR = 23.3 for rs4803219; **Supplementary Table 3**). We also performed LD and haplotype analyses with seven SNPs. These SNPs were in strong LD, and the risk haplotype showed a level of association similar to those of individual SNPs ($P = 1.35 \times 10^{-25}$, OR = 11.1; 95% CI = 6.6–18.6) (**Table 2**). These results suggest that the association with NVR was primarily driven by one of these SNPs.

Table 2 Association analysis of response to treatment by *IL28B* haplotype

SNP							Frequencies			
rs8105790	rs11881222	rs8103142	rs28416813	rs4803219	rs8099917	rs7248668	NVR group	VR group	*P* value	OR (95% CI)
T	A	T	C	C	T	G	0.543	0.942	1.81×10^{-32}	0.1 (0.04–0.12)
C	G	C	G	T	G	A	0.387	0.054	1.35×10^{-25}	11.1 (6.6–18.6)

Association analysis of haplotypes consisting of seven SNPs with response to PEG-IFN-α/RBV treatment in 314 Japanese patients with HCV. Boldface letters: rs11881222 (third intron); rs8103142 (third exon).

Table 3 Factors associated with NVR by logistic regression model

Factors	Odds ratio	95% CI	*P* value
rs8099917 (G allele)	37.68	16.71–83.85	<0.0001
Age	1.02	0.98–1.07	0.292
Gender (Female)	3.32	1.49–7.39	0.003
Re-treatment[a]	1.12	0.55–2.33	0.750
Platelet count	0.93	0.87–1.01	0.080
Aminotransferase level	1.00	0.99–1.00	0.735
Fibrosis stage[20]	1.10	0.73–1.66	0.658
HCV-RNA level	1.01	0.99–1.02	0.139

[a]Re-treatment, non-response to previous treatment with interferon-α (plus RBV).

To examine the relative contribution of factors associated with NVR, we used a logistic regression model. One tagging SNP located within *IL28B* (minor allele of rs8099917) was the most significant factor for predicting NVR, followed by gender (**Table 3**). Clinically, viral factors such as HCV genotype and HCV RNA level are important for the outcome of PEG-IFN-α/RBV therapy. Indeed, mean HCV-RNA level was significantly lower in SVR (SVR versus TVR, $P = 0.002$; SVR versus NVR, $P = 0.016$; **Supplementary Table 4**). Mean platelet count and the proportion of mild fibrosis (F1–F2) were significantly higher in SVR than in NVR.

Real-time quantitative PCR assays in peripheral blood mononuclear cells revealed a significantly lower level of *IL28* mRNA expression in individuals with the minor alleles (**Fig. 3**), suggesting that variant(s) regulating *IL28* expression is associated with a response to PEG-IFN-α/RBV treatment. *IL28B* encodes a cytokine distantly related to type I (α and β) interferons and the interleukin (IL)-10 family. This gene and *IL28A* and *IL29* (encoding IL-28A and IL-29, respectively) are three closely related cytokine genes that encode proteins known as type III IFNs (IFN-λs) and that form a cytokine gene cluster at chromosomal region 19q13 (ref. 16). The three cytokines are induced by viral infection and have antiviral activity[16,17]. All three interact with a heterodimeric class II cytokine receptor that consists of IL-10 receptor beta (IL10Rβ) and IL-28 receptor alpha (IL28Rα, encoded by *IL28RA*)[16,17], and they may serve as an alternative to type I IFNs in providing immunity to viral infection.

Notably, a recent report showed that the strong antiviral activity evoked by treating mice with TLR3 or TLR9 agonists was significantly reduced in both *IL28RA*$^{-/-}$ and *IFNAR*$^{-/-}$ mice, indicating that IFN-λ is important in mediating antiviral protection by ligands for TLR3 and TRL9 (ref. 18). IFN-λ induced a steady increase in the expression of a subset of IFN-stimulated genes, whereas IFN-α induced the same genes with more rapid and transient kinetics[19]. Therefore, it is possible that IFN-λ induces a slower but more sustained response that is important for TLR-mediated antiviral protection. This might be one of the ways that a genetic variant regulating *IL28* expression influences the response to PEG-IFN-α/RBV treatment. Further research will be required to fully understand the specific mechanism by which a genotype might affect the response to treatment.

In conclusion, the strongest associations with NVR were observed for seven SNPs, rs8105790, rs11881222, rs8103142, rs28416813, rs4803219, rs8099917 and rs7248668, that are located in the downstream flanking region, the third intron, the third exon, the first intron and the upstream flanking region of *IL28B*. Further studies following our report of this robust genetic association to NVR may make it possible to develop a pre-treatment predictor of which individuals are likely to respond to PEG-IFN-α/RBV treatment. This would remove the need for the initial 12–24 weeks of treatment that is currently used as a basis for a clinical decision about whether treatment should be continued. That would allow better targeting of PEG-IFN-α/RBV

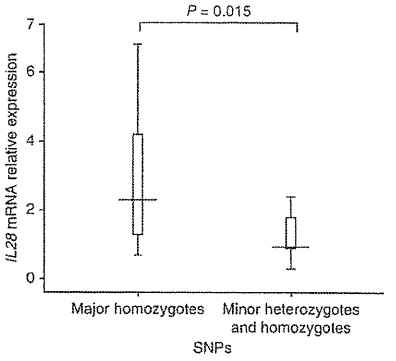

Figure 3 Quantification of *IL28* mRNA expression. The expression level of *IL28* genes was determined by real-time quantitative RT-PCR using RNA purified from peripheral blood mononuclear cells. Distribution of relative gene expression levels was compared between the individuals homozygous for major alleles ($n = 10$) and the heterozygous or homozygous individuals carrying minor alleles ($n = 10$) of rs8099917 by using the Mann-Whitney *U*-test. The bars indicate the median. All samples were obtained from HCV-infected patients before PEG-IFN-α/RBV therapy.

treatment, avoiding the unpleasant side effects that commonly accompany the treatment where it is unlikely to be beneficial, and reduce overall treatment costs. Because of the small number of samples in this study, we plan to conduct a further prospective multicenter study to establish these SNPs as a clinically useful marker.

METHODS

Methods and any associated references are available in the online version of the paper at http://www.nature.com/naturegenetics/.

Note: Supplementary information is available on the Nature Genetics website.

ACKNOWLEDGMENTS

This study was supported by a grant-in-aid from the Ministry of Health, Labour, and Welfare of Japan (H19-kannen-013). This study is based on 15 multicenter hospitals throughout Japan, in the Hokkaido area (Hokkaido University Hospital), Kanto area (Saitama University Hospital; Konodai Hospital; Musashino Red Cross Hospital; Tokyo Medical and Dental University Hospital), Koshin area (Shinshu University Hospital; Kanazawa University Hospital), Tokai area (Nagoya City University Hospital), Kinki area (Kyoto Prefectural University of Medicine Hospital; National Hospital Organization Osaka National Hospital; Hyogo College of Medicine Hospital) and Chugoku/Shikoku area (Tottori University Hospital; Ehime University Hospital; Yamaguchi University Hospital; Kawasaki Medical College Hospital). We thank Y. Uehara-Shibata, Y. Ogasawara, Y. Ishibashi and M. Yamaoka-Sageshima (Tokyo University) for technical assistance; A. Matsumoto (Shinshu), K. Naiki (Saitama), K. Nishimura (Kyoto), H. Enomoto (Hyogo), K. Oyama (Tottori) and the Ochanomizu Liver Conference Study Group for collecting samples; M. Watanabe (Tokyo Medical and Dental University), S. Kaneko (Kanazawa University) and M. Onji (Ehime University) for their advice throughout the study; and H. Ito (Aichi Cancer Center) for conducting statistical analyses.

AUTHOR CONTRIBUTIONS

Study design and discussion: Y.T., N.N., N.M., K.T., M.M.; sample collection: Y.T., M.K., K.M., N.S., M.N., M.K., K.H., S.H., Y.I., E.M., E.T., S.M., Y.M., M.H., A.S., Y.H., S.N., I.S., M.I., K.I., K.Y., F.S., N.I.; genotyping: N.N.; statistical analysis: N.N., A.K., K.I.; quantitative RT-PCR: M.S.; manuscript writing: Y.T., N.N., K.T., M.M.

Published online at http://www.nature.com/naturegenetics/.
Reprints and permissions information is available online at http://npg.nature.com/reprintsandpermissions/.

1. Ray Kim, W. Global epidemiology and burden of hepatitis C. *Microbes Infect.* 4, 1219–1225 (2002).
2. Manns, M.P. *et al.* Peginterferon alfa-2b plus ribavirin compared with interferon alfa-2b plus ribavirin for initial treatment of chronic hepatitis C: a randomised trial. *Lancet* **358**, 958–965 (2001).

3. Fried, M.W. *et al.* Peginterferon alfa-2a plus ribavirin for chronic hepatitis C virus infection. *N. Engl. J. Med.* **347**, 975–982 (2002).
4. Hadziyannis, S.J. *et al.* Peginterferon-alpha2a and ribavirin combination therapy in chronic hepatitis C: a randomized study of treatment duration and ribavirin dose. *Ann. Intern. Med.* **140**, 346–355 (2004).
5. Bruno, S. *et al.* Peginterferon alfa-2b plus ribavirin for naive patients with genotype 1 chronic hepatitis C: a randomized controlled trial. *J. Hepatol.* **41**, 474–481 (2004).
6. Sezaki, H. *et al.* Poor response to pegylated interferon and ribavirin in older women infected with hepatitis C virus of genotype 1b in high viral loads. *Dig. Dis. Sci.* **54**, 1317–1324 (2009).
7. Fried, M.W. Side effects of therapy of hepatitis C and their management. *Hepatology* **36**, S237–S244 (2002).
8. Pascu, M. *et al.* Sustained virological response in hepatitis C virus type 1b infected patients is predicted by the number of mutations within the NS5A-ISDR: a meta-analysis focused on geographical differences. *Gut* **53**, 1345–1351 (2004).
9. Shirakawa, H. *et al.* Pretreatment prediction of virological response to peginterferon plus ribavirin therapy in chronic hepatitis C patients using viral and host factors. *Hepatology* **48**, 1753–1760 (2008).
10. Akuta, N. *et al.* Predictive factors of early and sustained responses to peginterferon plus ribavirin combination therapy in Japanese patients infected with hepatitis C virus genotype 1b: amino acid substitutions in the core region and low-density lipoprotein cholesterol levels. *J. Hepatol.* **46**, 403–410 (2007).
11. Walsh, M.J. *et al.* Non-response to antiviral therapy is associated with obesity and increased hepatic expression of suppressor of cytokine signalling 3 (SOCS-3) in patients with chronic hepatitis C, viral genotype 1. *Gut* **55**, 529–535 (2006).
12. Gao, B., Hong, F. & Radaeva, S. Host factors and failure of interferon-alpha treatment in hepatitis C virus. *Hepatology* **39**, 880–890 (2004).
13. Matsuyama, N. *et al.* The dinucleotide microsatellite polymorphism of the IFNAR1 gene promoter correlates with responsiveness of hepatitis C patients to interferon. *Hepatol. Res.* **25**, 221–225 (2003).
14. Tsukada, H. *et al.* A polymorphism in MAPKAPK3 affects response to interferon therapy for chronic hepatitis C. *Gastroenterology* **136**, 1796–1805 (2009).
15. Nishida, N. *et al.* Evaluating the performance of Affymetrix SNP Array 6.0 platform with 400 Japanese individuals. *BMC Genomics* **9**, 431 (2008).
16. Kotenko, S.V. *et al.* IFN-λs mediate antiviral protection through a distinct class II cytokine receptor complex. *Nat. Immunol.* **4**, 69–77 (2003).
17. Sheppard, P. *et al.* IL-28, IL-29 and their class II cytokine receptor IL-28R. *Nat. Immunol.* **4**, 63–68 (2003).
18. Ank, N. *et al.* An important role for type III interferon (IFN-lambda/IL-28) in TLR-induced antiviral activity. *J. Immunol.* **180**, 2474–2485 (2008).
19. Marcello, T. *et al.* Interferons alpha and lambda inhibit hepatitis C virus replication with distinct signal transduction and gene regulation kinetics. *Gastroenterology* **131**, 1887–1898 (2006).
20. Desmet, V.J., Gerber, M., Hoofnagle, J.H., Manns, M. & Scheuer, P.J. Classification of chronic hepatitis: diagnosis, grading and staging. *Hepatology* **19**, 1513–1520 (1994).

ONLINE METHODS

Study cohorts. From April 2007 to April 2009, samples were obtained from 314 patients with chronic HCV (genotype 1) infection who were treated at 15 multicenter hospitals (liver units with hepatologists) throughout Japan. Each patient was treated with PEG-IFN-α2b (1.5 μg per kg body weight (μg/kg) subcutaneously once a week) or PEG-IFN-α2a (180 μg/kg once a week) plus RBV (600–1,000 mg daily depending on body weight). As a reduction in the dose of PEG-IFN-α and RBV can contribute to a less sustained virological response[21], only patients with an adherence of >80% dose for both drugs during the first 12 weeks were included in this study. HBsAg-positive and/or anti-HIV–positive individuals were excluded from this study.

NVR (seen in ~20% of total treated patients) was defined as less than a 2-log-unit decline in the serum level of HCV RNA from the pre-treatment baseline value within the first 12 weeks and detectable viremia 24 weeks after treatment. VR was defined as the achievement of SVR or transient TVR in this study; SVR was defined as undetectable HCV RNA in serum 6 months after the end of treatment, whereas TVR was defined as a reappearance of HCV RNA in serum after treatment was discontinued in a patient who had undetectable HCV RNA during the therapy or on completion of the therapy. Of 878 patients with HCV genotype 1 treated by PEG-IFN-α/RBV at 14 hospitals, only 114 (13.0%) met the criteria for NVR in this study. For the GWAS stage of the study, a case-control study was conducted comparing individuals with NVR (82 individuals) and VR (72 individuals). For the replication stage, an independent cohort of samples from 172 Japanese patients with HCV genotype 1, including 50 with NVR and 122 with VR, was obtained from an independent cohort study at Tokyo Medical and Dental University Hospital (Ochanomizu Liver Conference Study Group) and Musashino Red Cross Hospital. Clinical data from the combined cohorts, with a total of 140 SVR, 46 TVR and 128 NVR patients, are shown in **Supplementary Table 4**.

Informed consent was obtained from each patient who participated in the study. The study protocol conforms to the relevant ethical guidelines as reflected in *a priori* approval by the ethics committees of all the participating universities and hospitals.

SNP genotyping and data cleaning. In the GWAS stage, we genotyped 154 Japanese patients with HCV receiving PEG-IFN-α/RBV treatment using the Affymetrix Genome-Wide Human SNP Array 6.0 according to the manufacturer's instructions. After exclusion of 4 NVR samples and 8 SVR samples with QC call rates <95%, the remaining 142 samples were recalled using the Birdseed version 3 software (Affymetrix). The average overall call rate of 78 NVR and 64 VR samples reached 99.46% and 99.46%, respectively. We then applied the following thresholds for QC in data cleaning: SNP call rate ≥95% for all samples, MAF ≥1% for all samples and HWE P value ≥0.001 for VR group[22,23]. A total of 621,220 SNPs on autosomal chromosomes passed the QC filters and were used for association analysis. All cluster plots for the SNPs showing $P < 0.001$ in association analyses by comparing allele frequencies in NVR and VR groups were checked by visual inspection. SNPs with ambiguous genotype calls were excluded. **Supplementary Table 5** shows SNPs that might be weakly associated with NVR ($P < 10^{-4}$).

Although the 12 samples noted above were excluded from the GWAS stage by data cleaning, their quality was good enough for the SNP typing in the replication study, and thus they were included in the replication stage. In the subsequent replication stage with high-density association mapping, SNP genotyping in the independent set of 172 patients was completed using the DigiTag2 assay[24] and direct sequencing using the Applied Biosystems 3730 DNA Analyzer (Applied Biosystems). In addition, strongly associated SNPs identified in the GWAS stage were also genotyped for the GWAS samples using the DigiTag2 assay, and the results were 100% concordant to those from the GWAS platform.

Screening for new polymorphisms. To determine possible genomic variants in the region of *IL28B* and its promoter, we sequenced the 3.3-kb region in a total of 48 Japanese patients with HCV (28 NVR and 20 VR). We selected 7 samples from NVR patients who were minor allele homozygotes for 2 SNPs (rs12980275 and rs8099917), 11 samples from NVR and 10 samples from VR heterozygotes, and 10 samples from NVR and 10 samples from VR major allele homozygotes. The sequencing primers were designed using the Visual OMP Nucleic Acid software (**Supplementary Table 6**). PCR was carried using TaKaRa LA *Taq* polymerase (Takara Biochemicals) under the following thermal cycler conditions: stage 1, 94 °C for 1 min; stage 2, 98 °C for 10 s, 68 °C for 15 min, for a total of 30 cycles; stage 3, 72 °C for 10 min. A 50-μl PCR analysis was performed using 2.5 U TaKaRa LA *Taq* with 1× LA PCR buffer II, 0.4 mM dNTP, 10 pmol of each primer and 10 ng of genomic DNA. For sequencing, 7.0 μl of the PCR products were incubated with 3 μl of Exonuclease I/Shrimp Alkali Phosphatase (Takara Biochemicals) first for 90 min at 37 °C and then for another 10 min at 80 °C. Sequencing reactions were performed with the use of a BigDye Terminator Cycle Sequencing FS Ready Reaction Kit (Applied Biosystems). After purification with MultiScreen-HV (Millipore) and Sephadex G-50 Fine (GE Healthcare UK Ltd.), the reaction products were applied to the Applied Biosystems 3730 DNA Analyzer.

In the variation screening, three SNPs (rs8103142, rs28416813 and rs4803219) and a few infrequent variations were detected. We then typed these SNPs in all of the 314 patients.

Statistical analysis. The observed association between a SNP and response to PEG-IFN-α/RBV treatment was assessed by χ^2 test with a two-by-two contingency table in three genetic models: allele frequency model, dominant-effect model and recessive-effect model. SNPs on the X chromosome were removed because gender was not matched between the NVR group and the VR group. A total of 621,220 SNPs passed the QC filters in the GWAS stage; therefore, significance levels after the Bonferroni correction for multiple testing were $P = 8.05 \times 10^{-8}$ (0.05/621,220) in the GWAS stage and $P = 0.0031$(0.05/16) in the replication stage. None of the 16 markers genotyped in the replication stage showed deviations from Hardy-Weinberg equilibrium in the VR group ($P > 0.05$).

The inflation factor λ was estimated based on the median χ^2 and revealed to be 1.029 (median) and 1.011 (mean), suggesting that the population substructure should not have any substantial effect on the statistical analysis (**Supplementary Fig. 1**). In addition, the principal component analysis on the 142 patients (78 NVR samples and 64 VR samples) analyzed in the GWAS stage together with the HapMap samples also revealed that the effect of population stratification was negligible (**Supplementary Fig. 2**).

For the replication study and the high-density association mapping, 16 SNPs were selected from the region of ~40 kb (chr. 9, nucleotide positions 44421319–44461718; build 35) containing the significantly associated SNPs (rs12980275 and rs8099917) in the GWAS stage by analyzing, using Haploview software, LD and haplotype structure based on the HapMap data for individuals of Japanese descent. These SNPs included tagging SNPs estimated on the basis of haplotype blocks, SNPs located within the *IL28B* and *IL28A* genes (rs11881222 and rs576832, respectively) and the significantly associated SNPs identified in the GWAS stage (**Supplementary Table 1**). On the basis of the genotype data from the total of 314 patients in the GWAS stage and replication stages, haplotype blocks were estimated using the four-gamete rule, and three blocks were observed (**Fig. 2**). Association of haplotype with response to PEG-IFN-α/RBV treatment was analyzed using Haploview software.

The logistic regression model was used to assess the factors associated with NVR. STATA 10 (Statacorp LP) was used for all analysis. Age, platelet count, and aminotransferase (ALT) and HCV-RNA levels were applied as continuous variables.

Real-time quantitative RT-PCR for *IL28* gene. A layer of mononuclear cells was collected via Ficoll from peripheral blood. Total RNA was isolated using the RNeasy Mini Kit and the RNase-Free DNase Set (Qiagen) according to the manufacturer's protocol. First-strand cDNA was synthesized using SuperScript II reverse transcriptase with Oligo $(dT)_{12-18}$ primer (Invitrogen). The relative quantification of the target gene was determined using Custom TaqMan Gene Expression Assays, and the expression of glyceraldehyde-3-phosphate dehydrogenase was used to normalize the gene expression level (Applied Biosystems) according to the manufacturer's protocol. The data were analyzed by the $2[-\Delta\Delta C_t]$ method using Sequence Detector version 1.7 software (Applied Biosystems). A standard curve was prepared by serial tenfold dilutions of

doi:10.1038/ng.449

human cDNA. The curve was linear over 7 logs with a correlation coefficient of 0.998. The specific detection of *IL28B* in real-time PCR is hard to establish, because the nucleotide differences between *IL28A* and *IL28B* consist of only 9 nucleotides scattered throughout the gene. Primers and probes are designed for the *IL28* gene (**Supplementary Table 6**).

URLs. The results of the present GWAS have been registered at a public database: https://gwas.lifesciencedb.jp/cgi-bin/gwasdb/gwas_top.cgi.

21. McHutchison, J.G. *et al.* Adherence to combination therapy enhances sustained response in genotype-1-infected patients with chronic hepatitis C. *Gastroenterology* **123**, 1061–1069 (2002).
22. Miyagawa, T. *et al.* Variant between *CPT1B* and *CHKB* associated with susceptibility to narcolepsy. *Nat. Genet.* **40**, 1324–1328 (2008).
23. Miyagawa, T. *et al.* Appropriate data cleaning methods for genome-wide association study. *J. Hum. Genet.* **53**, 886–893 (2008).
24. Nishida, N., Tanabe, T., Takasu, M., Suyama, A. & Tokunaga, K. Interferons alpha and lambda inhibit hepatitis C virus replication with distinct signal transduction and gene regulation kinetics. *Gastroenterology* **131**, 1887–1898 (2006).

ELSEVIER

Journal of Hepatology 51 (2009) 1046–1054

Journal of Hepatology

www.elsevier.com/locate/jhep

Absence of viral interference and different susceptibility to interferon between hepatitis B virus and hepatitis C virus in human hepatocyte chimeric mice☆

Nobuhiko Hiraga[1,2], Michio Imamura[1,2], Tsuyoshi Hatakeyama[1], Shosuke Kitamura[1], Fukiko Mitsui[1,b], Shinji Tanaka[1], Masataka Tsuge[1,2], Shoichi Takahashi[1,2], Hiromi Abe[2,3], Toshiro Maekawa[2,3], Hidenori Ochi[2,3], Chise Tateno[2,4], Katsutoshi Yoshizato[2,4,5], Takaji Wakita[6], Kazuaki Chayama[1,2,3,*]

[1]*Department of Medicine and Molecular Science, Division of Frontier Medical Science, Programs for Biomedical Research, Graduate School of Biomedical Sciences, Hiroshima University, 1-2-3 Kasumi, Minami-ku, Hiroshima 734-8551, Japan*

[2]*Liver Research Project Center, Hiroshima University, Hiroshima, Japan*

[3]*Laboratory for Liver Diseases, SNP Research Center, The Institute of Physical and Chemical Research (RIKEN), Yokohama, Japan*

[4]*PhoenixBio Co., Ltd., Higashihiroshima, Japan*

[5]*Osaka City University Graduate School of Medicine, Osaka, Japan*

[6]*Department of Virology II, National Institute of Infectious Diseases, Shinjuku-ku, Japan*

***Background/Aims*: Both hepatitis B virus (HBV) and hepatitis C virus (HCV) replicate in the liver and show resistance against innate immunity and interferon (IFN) treatment. Whether there is interference between these two viruses is still controversial. We investigated the interference between these two viruses and the mode of resistance against IFN.**

***Methods*: We performed infection experiments with either or both of the two hepatitis viruses in human hepatocyte chimeric mice. Huh7 cell lines with stable production of HBV were also established and transfected with HCV JFH1 clone. Mice and cell lines were treated with IFN. The viral levels in mice sera and culture supernatants and messenger RNA levels of IFN-stimulated genes were measured.**

***Results*: No apparent interference between the two viruses was seen *in vivo*. Only a small (0.3 log) reduction in serum HBV and a rapid reduction in HCV were observed after IFN treatment, regardless of infection with the other virus. In *in vitro* studies, no interference between the two viruses was observed. The effect of IFN on each virus was not affected by the presence of the other virus. IFN-induced reductions of viruses in culture supernatants were similar to those in *in vivo* study.**

***Conclusions*: No interference between the two hepatitis viruses exists in the liver in the absence of hepatitis. The mechanisms of IFN resistance of the two viruses target different areas of the IFN system.**

Keywords: **Superinfection; JFH-1; IFN-stimulated genes**

Received 4 February 2009; received in revised form 14 July 2009; accepted 15 July 2009; available online 23 September 2009

Associate Editor: F. Zoulim

☆ C.T. and K.Y. are employees of PhoenixBio Co. Ltd., Higashihiroshima, Japan. The other authors who have taken part in this study declared that they do not have anything to disclose regarding funding from industry or conflict of interest with respect to this manuscript.

* Corresponding author. Tel.: +81 82 2575190; fax: +81 82 2556220.

E-mail address: chayama@hiroshima-u.ac.jp (K. Chayama).

Abbreviations: GAPDH, glyceraldehydes-3-phosphate dehydrogenase; HBeAg, hepatitis B e antigen; HBsAg, hepatitis B surface antigen; HBV, hepatitis B virus; HCV, hepatitis C virus; IFN, interferon; OAS, 2′,5′-oligoadenylate synthetase; PCR, polymerase chain reaction; SCID, severe combined immunodeficiency; uPA, urokinase-type plasminogen activator.

0168-8278/$36.00 © 2009 European Association for the Study of the Liver. Published by Elsevier B.V. All rights reserved.
doi:10.1016/j.jhep.2009.09.002

1. Introduction

Both hepatitis B virus (HBV) and hepatitis C virus (HCV) infections are serious health problems worldwide. More than 350 million people are infected with HBV, and more than 170 million people are infected with HCV [1,2]. Both types of hepatitis viruses result in the development of chronic liver infection and lead to death due to liver failure and hepatocellular carcinoma [3]. To date, interferon (IFN) remains one of the most important drugs available for the treatment of both types of hepatitis viral infections. Although it is assumed that IFN suppresses viral replication through the effect of IFN-induced gene products such as mixovirus resistance protein A (MxA), RNA-dependent protein kinase (PKR), and 2′,5′-oligoadenylate synthetase (OAS) [4], the precise mechanism of action of these proteins on both hepatitis viruses are unknown.

Coinfection with both viruses leads to a rapid and severe progression of chronic liver disease [5], with a higher risk of hepatocellular carcinoma [6]. Currently, there is a debate about whether or not there is interference between the two hepatitis viruses, with some favoring such interference [7] and others arguing against such a concept [8]. A number of mechanisms can cause interference between viruses. A major mechanism of interference is induction of IFN by one virus to prevent replication of the second virus; however, viruses develop their own strategies to resist the effect of IFN. In clinical practice, practitioners often perceive that reduction of HBV in serum by IFN therapy is poorer compared with HCV. HCV levels in sera of IFN-treated patients decrease relatively rapidly, and a proportion of patients eventually show complete eradication of the virus. Furthermore, the recent use of pegylated IFN (PEG-IFN) in combination with ribavirin has improved the eradication rate [9]. Eradication of HBV by IFN, however, is usually difficult, even when using IFN combined with ribavirin [10].

The mechanisms developed by viruses to resist host innate immunity, including IFN signaling, are well established in some viruses. Such mechanisms involve interruption of IFN signaling by interacting molecules that transduce the signal from the IFN receptor through the Janus kinase (Jak) signal transducer and activator of transcription (STAT) pathway [4]. Viral proteins of paramixoviruses, for example, inhibit IFN signaling [11]. Several studies have also examined the mechanisms by which HCV resists the host immune system. These include degradation of Cardif adaptor protein by NS3A/4 protease [12]. Generally, expression of HCV protein is associated with inhibition of STAT1 function independent of STAT tyrosine phosphorylation [13]. Additionally, expression of the HCV core protein in cultured cells is associated with increased expression levels of the suppressor of cytokine signaling 3 (SOCS-3) [14]. The NS5A and E2 proteins are both inhibitors of PKR [15]. These strong actions of HCV against innate immunity are consistent with the high chronicity rate of the virus. IFN, however, effectively reduces HCV replicon in Huh7 cells [16], suggesting that the virus has little potential to disturb the actions of IFN.

In contrast to HCV, the mechanisms of IFN resistance by HBV are poorly understood. To date, only a few studies have reported the molecular mechanisms of HBV resistance against the actions of IFN. The HBV-related resistance to IFN, for example, involves upregulation of protein phosphatase 2A (PP2A) as the primary event, which subsequently leads to inhibition of protein arginine methyltransferase 1 (PRMT1) and reduced STAT1 methylation [17]. In addition to these molecular mechanisms, microarray analyses of serial liver biopsies of experimentally infected chimpanzees showed striking differences in the early immune responses to HBV and HCV. HCV, for example, induced early changes in the expression of many intrahepatic genes, including genes involved in type 1 IFN response [18], whereas HBV did not induce any detectable changes in the expression of intrahepatic genes in the first weeks of infection [19].

HBV–HCV double infection is a good model to use for assessment of the mechanism of IFN resistance by these two viruses because one can test the effect of IFN on one virus in the presence of the other virus. Recently, Bellecave et al. [20] established a novel *in vitro* model system in Huh7 cells that allowed the analysis of both viruses in a replicating context and reported the absence of direct viral interference. To this end, we used human hepatocyte chimeric mice and cell culture systems in the present study. The results showed that the presence of HBV does not affect the actions of IFN on HCV and vice versa. These results suggest the lack of interference between the two viruses in liver cells and indicate that the reported interference between the two viruses might be via inflammation including death of infected cells by cytotoxic T cells, cytokines including IFN-α and IFN-β, and interleukins produced by hepatocytes and infiltrating T cells.

2. Materials and methods

2.1. Transfection of Huh7 cells with HBV DNA and HCV RNA

Huh7 cells were grown in Dulbecco's modified Eagle's medium supplemented with 10% (v/v) fetal bovine serum at 37 °C and under 5% CO_2. Cloning of HBV DNA and the plasmid construction were performed as described previously [21]. For production of stably transfected cell lines, Huh7 cells were seeded onto 90-mm-diameter culture dishes. Twenty micrograms of the plasmid pTRE-HB-wt [21] was transfected by the calcium phosphate precipitation method. Twenty-four hours after transfection, the cells were split and cultured in Hygromycin B-DMEM selection medium (300 μg/ml; Invitrogen Japan K.K., Osaka, Japan), while 50 colonies were isolated and cultured for identification of virus-producing cell lines. Clones positive

for both hepatitis B surface antigen (HBsAg) and hepatitis B e antigen (HBeAg) were selected and further analyzed for production of HBV particles. Finally, three cell lines that produced more than 10^5 copies per milliliter of HBV DNA in supernatant were selected and used for further experiments.

For transfection with HCV RNA, we used pJFH1, which contains the complementary DNA of full-length genotype 2a HCV clone JFH1 downstream of the T7 promoter [22]. *In vitro* synthesis of HCV RNA and electroporation into Huh7 cells were performed as described previously [22,23]. Briefly, cells were treated with trypsin, washed twice with ice-cold RNase-free phosphate-buffered saline, and resuspended in Opti-MEM I (Invitrogen, Carlsbad, CA, USA) at a final concentration of 7.5×10^6 cells per milliliter. Then, 10 μg of HCV RNA to be electroporated was mixed with 0.4 mL of cell suspension and subjected to an electric pulse (950 μF and 260 V) using the Gene Pulser II Electroporation System (Bio-Rad, Hercules, CA, USA). After electroporation, the cell suspension was left for 5 min at room temperature and then incubated under normal culture conditions in a 10-cm-diameter cell culture dish.

2.2. Generation of human hepatocyte chimeric mice

Generation of the urokinase-type plasminogen activator $(uPA)^{+/+}$ and severe combined immunodeficiency $(SCID)^{+/+}$ mice and transplantation of human hepatocytes were performed as described recently by our group [21,23,24]. All mice were transplanted with frozen human hepatocytes obtained from the same donor. Infection, extraction of serum samples, and euthanasia were performed under ether anesthesia. The concentration of serum human serum albumin, which correlates with the repopulation index [24], was measured in mice as described previously [21]. All animal protocols described in this study were performed in accordance with the guidelines of the local committee for animal experiments. The experimental protocol was approved by the Ethics Review Committee for Animal Experimentation of Graduate School of Biomedical Sciences, Hiroshima University, Hiroshima, Japan.

2.3. Human serum samples

Human serum samples containing high titers of either HBV DNA (5.3×10^6 copies per milliliter) or genotype 1b HCV (2.2×10^6 copies per milliliter) were obtained from patients with chronic hepatitis with a written informed consent. The individual serum samples were divided into small aliquots and separately stored in liquid nitrogen until use. Chimeric mice were injected intravenously with 50 μL of either HBV- or HCV-positive human serum. Some mice were injected with HBV-positive human serum at 6 weeks after injection of HCV-positive human serum.

2.4. Analysis of HBV and HCV

HBsAg and HBeAg in culture supernatants were measured by commercially available enzyme-linked immunosorbent assay (ELISA) kits (Abbott Japan, Osaka, Japan). DNA was extracted from these samples by SMITEST (Genome Science Laboratories, Tokyo, Japan) and dissolved in 20 μL H_2O [21,25]. RNA was extracted from serum samples by Sepa Gene RV-R (Sankojunyaku, Tokyo), dissolved in 8.8 μL RNase-free H_2O, and reverse transcribed using random primer (Takara Bio Inc., Shiga, Japan) and M-MLV reverse transcriptase (ReverTra Ace, TOYOBO Co., Osaka, Japan) in a 20-μL reaction mixture according to the instructions provided by the manufacturer [23]. HCV core antigen in the culture medium was detected with HCV Ag assay (Ortho-Clinical Diagnostics, Rochester, NY, USA).

2.5. RNA extraction and measurement of mRNAs of interferon-induced genes by quantitative reverse transcription-polymerase chain reaction

Total RNA was extracted from cell lines using the RNeasy Mini Kit (Qiagen, Valencia, CA, USA). One nanogram of each RNA was reverse transcribed with ReverseTra Ace (TOYOBO Co.) and Random Primer (Takara Bio, Kyoto, Japan). We quantified the transcripts for MxA, OAS, and PKR. Amplification and detection were performed using ABI PRISM 7300 (Applied Biosystems, Foster City, CA, USA). Results were normalized to the transcript levels of glyceraldehydes-3-phosphate dehydrogenase (GAPDH).

2.6. Statistical analysis

Changes in HBV DNA and HCV RNA in mice sera were compared by Mann–Whitney test and unpaired t test. Differences in HBV DNA and HCV core antigen in mice sera and culture supernatants were analyzed by one-way analysis of variance followed by Scheffe's test. A P value of <0.05 was considered statistically significant.

3. Results

3.1. Infection of chimeric mouse with HBV and HCV and susceptibility to interferon

To investigate the interference between HBV and HCV and to examine the effect of IFN on both of these two viruses *in vivo*, we used six human chimeric mice. Each of six mice was inoculated intravenously with 50 μL of serum samples obtained from either HBV- or HCV-positive patients. The median HBV DNA level in HBV-positive serum-inoculated mice was 1.4×10^8 copies per milliliter (range: 5.3×10^6–3.6×10^9 copies per milliliter) at 6 weeks after inoculation (Fig. 1A), similar to our recent observation [21]. Similarly, the median HCV RNA level in HCV-positive human serum-inoculated mice was 1.0×10^7 copies per milliliter (range: 1.2×10^6–0.8×10^7 copies per milliliter) at 4 weeks after inoculation (Fig. 1B), as reported recently by our group [23]. Six weeks after inoculation, three of six HBV- or HCV-infected mice were treated daily with 7000 IU/g per day of intramuscular IFN-α for 2 weeks. Treatment resulted in a decrease of only 0.3 log in mice serum HBV DNA level compared to that in mice without treatment (Fig. 1A). In contrast, the same therapy resulted in a rapid decrease in HCV RNA to undetectable levels, as confirmed by quantitative polymerase chain reaction (PCR; Fig 1B).

To investigate the direct interference of the two viruses, we performed double-infection experiments. Ten chimeric mice were first inoculated intravenously with 50 μL of HCV-positive human serum samples. Six weeks after HCV infection when the mice developed HCV viremia, 50 μL of HBV-positive human serum samples were inoculated intravenously in 5 of 10 HCV-infected mice. All five mice became positive for both HBV and HCV at 2 weeks after HBV infection. No significant decrease in HCV RNA levels was observed in these superinfected mice before or after the development of HBV viremia (Fig. 2A). After HBV infection, there was no apparent decrease in HCV titer (Fig. 2B). Moreover, HBV DNA level in HBV–HCV-coinfected mice was comparable with that of only HBV-infected mice (Fig. 2B). These results sug-

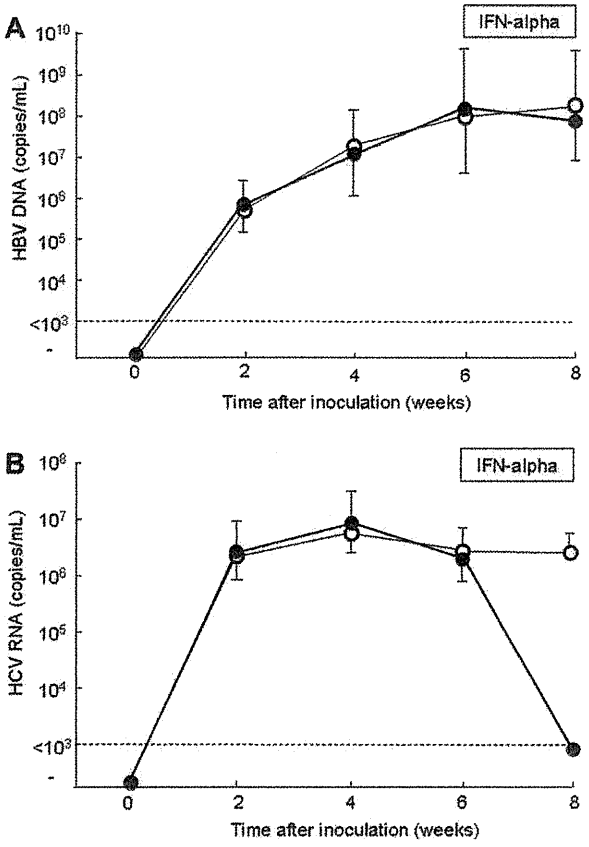

Fig. 1. Changes in serum virus titers in mice inoculated with hepatitis B virus (HBV) – positive or hepatitis C virus (HCV) – positive human serum samples. (A) HBV DNA levels in six mice inoculated with HBV-positive serum samples. (B) HCV RNA levels in six mice inoculated with HCV-positive serum samples. Six weeks after inoculation, three of six mice were treated daily with (closed circles) or without (open circles) 7000 IU/g per day of interferon-alpha intramuscularly for 2 weeks. Mice serum samples were extracted every 2 weeks after inoculation. Data are mean plus or minus standard deviation ($n = 3$). The horizontal dashed line represents the detection limit (10^3 copies per milliliter).

gest no interference between the two viruses in mice, which lack immunocytes known to cause hepatitis.

To further investigate if infection with either of the two hepatitis viruses alters the effect of IFN against the other virus, three HBV–HCV-coinfected mice were treated with IFN-α (Fig. 3A). Such treatment resulted in a rapid decrease in HCV RNA in all mice to undetectable levels as confirmed by quantitative PCR (Fig. 3B). In contrast, no significant decrease in HBV DNA titers was observed in these mice (Fig. 3B). These results are similar to the reduction of HCV RNA and HBV DNA in mice that were infected with either of these hepatitis viruses. These results indicate that HCV is more susceptible to IFN-α than HBV and that each virus does not alter the effect of IFN on the other virus. Because the effect of IFN on HCV was not disturbed by HBV, we assumed that HBV has no effect on the signal from IFN receptor to IFN-stimulated genes. It is possible, however, that HBV and HCV replicated in different cells in these mice. Because it was impossible to detect HCV protein and RNA in HCV-infected mouse liver by histologic examination, we performed *in vitro* experiments.

3.2. Production of both HBV- and HCV-producing cells and the effect of interferon

To investigate the effect of IFN on HBV and HCV *in vitro*, we created cell lines that produce both HBV and HCV. First, we established stable HBV-producing Huh7 cell lines. Three cell lines (Clone-39, -42, and -53) that produced HBsAg, HBeAg, and HBV DNA into the supernatant were selected (Table 1). These cell lines continuously produced HBV for more than 3 months (data not shown). Next, JFH1 RNA was transfected into these HBV-producing cell lines to produce both HBV DNA and HCV proteins into the supernatant. HBV DNA levels in the supernatants of these cell lines decreased in Clone-39, increased in Clone-42, and did not change in Clone-53 after JFH1 transfection (Fig. 4A). In contrast, HCV core antigen levels in the supernatants were higher in two of the three cell lines (Clone-39 and -42) than in Huh7 cells, and the level was not different in the remaining cell line (Clone-53) (Fig. 4B). These results indicate that the production of each of the two viruses does not disturb the replication of the other virus.

3.3. Effects of interferon on HBV and HCV in vitro

The effects of IFN on virus production in both HBV- and HCV-producing cell lines was examined by adding different amounts of IFN-α (0, 50, and 500 IU/mL) into the culture. The mRNA levels of intracellular IFN-stimulated genes such as MxA, OAS, and PKR increased in a dose-dependent manner in all three cell lines as well as in parental Huh7 cells (Fig. 5A). Following the addition of IFN, no apparent reduction of HBV was noted in the supernatant of HBV–HCV-cotransfected cell lines (Fig. 5B). In contrast, the levels of HCV core antigen in the supernatant decreased in all three cell lines treated with IFN, and the decrease was dose-dependent (Fig. 5C).

4. Discussion

Although IFN treatment for chronic HCV infection has improved with the advent of PEG-IFN, the rate of viral eradication remains unsatisfactory [9]. The mechanism responsible for failure of IFN to eradicate the virus completely must be clarified. To study the mechanism of viral resistance against IFN, analysis of viral interference may give us some hints because one of the major mechanisms of interference is through the action of IFN.

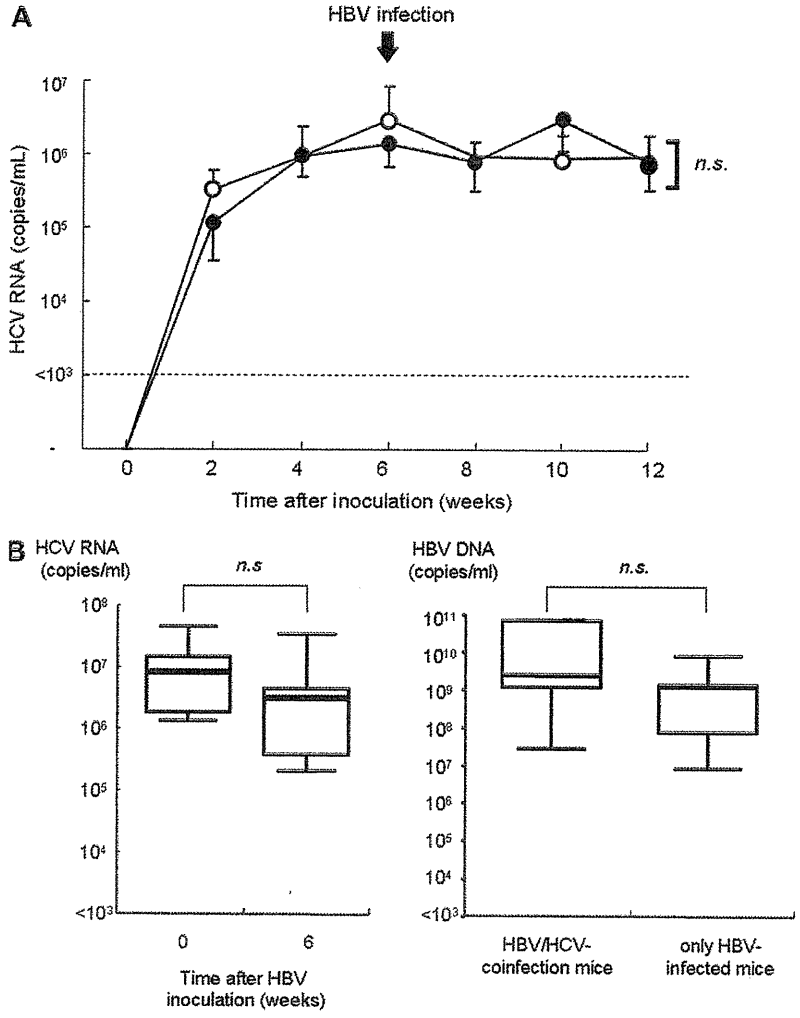

Fig. 2. Comparison of hepatitis C virus (HCV) and hepatitis B virus (HBV) titers in experimentally infected mice. (A) Ten mice were inoculated with HCV-positive serum samples. Six weeks after HCV infection, 5 of the 10 mice were inoculated with HBV-positive human serum samples (closed circles). The remaining five mice (open circles) did not receive HBV inoculation. Data are mean plus or minus standard deviation ($n = 3$). (B) Serum HCV RNA titers in five mice infected with HCV before and at 6 weeks after HBV superinfection (left panel). Serum HBV DNA titers in five mice coinfected with HBV and HCV were compared with those of five mice with HBV infection only (Fig. 1) at 12 weeks after HCV inoculation (right panel). In these box-and-whisker plots, lines within the boxes represent the median values; the upper and lower lines of the boxes represent the 25th and 75th percentiles, respectively.

Accumulation of mononuclear cells is usually seen in the livers of infected individuals, in association with the state of inflammation. It is thus difficult to examine the interference of hepatitis viruses in infection and replication in liver cells without taking into consideration the effect of these immune cells as well as the chemokines and cytokines produced by these cells. Instead, the present study was designed to examine the interference between HBV and HCV in an experimental setup lacking such inflammatory interferences. The SCID-based human hepatocyte chimeric mouse model is ideal for investigating such interaction. We expected either reduction of HCV after inoculation of HBV in HCV-infected mice or failure to develop HBV viremia or low-level HBV viremia in these mice due to viral interference; however, no reduction in HCV titers occurred in these mice, and HBV infection developed in a manner similar to that in naïve mice (Fig. 2). We thus confirmed that there is no interference between the two viruses in the absence of immune reaction via the infiltrating lymphocytes in the liver.

Wieland et al. reported that HBV did not induce any genes during entry or expansion in HBV-infected chimpanzee livers and suggested that HBV was a stealthy virus early in the infection [19]. Because no reduction in HCV was noted during and after the development of high-level HBV viremia, we assume that HBV escapes innate immunity via an excellent mechanism without